Tools to Study the Kinesin Mechanome Using Optical Tweezers

by

Ricardo González Rubio

B.S. Physics (Summa Cum Laude)
City College of the City University of New York

Submitted to the Department of Biological Engineering in Partial Fulfillment of the Requirements for the Degree of

Master of Science in Biological Engineering
at the
Massachusetts Institute of Technology

September 2009

Signature of Author.....
Department of Biological Engineering
July 1, 2009

Certified by.....
Matthew J. Lang
Associate Professor of Mechanical and Biological Engineering
Thesis Supervisor

Accepted by .....
Alan J. Grodzinsky
Professor of Electrical, Mechanical and Biological Engineering
Chairman, Department Committee on Graduate Students

Abstract

Molecular motors play an important role in driving some of the most complex and important tasks in biological systems, ranging from transcribing RNA from a DNA template (Polymerases) to muscle contraction (Myosin) and propelling bacteria (Flagellum). Key to the understanding of the fundamental principles and designs by which molecular motor function has been the kinesin family. Missing, however, is a clear understanding of the series of events that take place at the atomistic level when kinesin walks on a microtubule and generates force. Recent MD simulations have identified the force-generating mechanism in kinesin, the cover-neck bundle, and strongly suggest that the formation of the CNB by the N-terminal cover strand and the C-terminal neck linker of the motor head are responsible for force generation.

In this thesis we present tools developed in the Lang Laboratory to further elucidate the stepping motion and force generation mechanism of kinesin using Drosophila kinesin as a model system. We demonstrate the function of a force clamp specifically designed for the laboratory and show traces of WT kinesin walking under constant load. We also purified and tested kinesin mutants running under a force load. We present two assays specifically designed to study the interaction between kinesin and the last 10-18 C-terminal residues of α-β tubulin, the E-hook. We were unable to observe kinesin – e-hook interactions, such as those suggested by the formation of tethers, when the e-hook was bound to the surface. In the case of e-hook in solution, our results indicate that 2G kinesin was still functional and its stall force approximately 3 pN just as for the case when no e-hook is present.

We also propose ways that the work in this thesis can be expanded. The force clamp can be easily adapted to study novel kinesin mutants under constant load in 2D. In addition, the force clamp can be used to probe the kinesin - e-hook interactions by looking at kinesin walking over microtubules with cleaved e-hooks. The e-hook assays presented in this thesis can also be expanded to include higher concentrations of e-hook or be performed using labeled e-hook to assess single molecule interactions and concentrations.

Acknowledgments

I am extremely thankful to my advisor, Prof. Matthew J. Lang, for his all support and encouragement. I truly appreciate the guidance, words of advice and freedom to pursue my interests while in the laboratory. I really enjoyed the numerous hours spent alongside Prof. Lang running the optical trap. I also want to thank the members of the Lang Lab, both past and present, for their help with numerous aspects of this thesis. I am indebted to David Appleyard, Carlos Castro, Yongdae Shin, Ted Feldman, Marie Aubin-Tam, Matt Wohlever, and Mo Khalil not only for their help in preparing this thesis but also for their friendship and contributions to make the Lang Lab a wonderful place to work and learn.

I also want to thank all my friends, at M.I.T. and outside, for their continuous support and encouragement. I wish I had enough space to mention everyone's name. I want to specially thank Eddie Elthouky, Francisco Delgado, Salil Desai, David J. Quinn and Kristin Bernick, for stimulating conversations, many cups of coffee, and above all, their friendship. Also, a big thank you to the rest of my BE class.

Before joining the Biological Engineering Department, I spent some time working in the Fee Lab at the McGovern Institute. My experiences while there–and even after leaving–have contributed to my perseverance and success. I thank Prof. Michale S. Fee for his support in numerous occasions and welcoming me to his laboratory. I also want to thank Prof. Bence P. Olveczky for his unconditional support and encouragement to pursue my own interests.

Most importantly, I want to thank my family for always being there when I needed them the most. My father and mother, whom from the day I decided to study Physics, have always been a constant source of support and unconditional understanding. My brother, who is a graduate student in Biology at M.I.T., also played a role in helping me become a better biologist. Last, and most significantly, I need to thank my wife Anne for all she has done to make sure I always kept my priorities in place and giving me all her love and understanding. Without her support this thesis would have never been completed.

I am also thankful for the generous financial support provided by the Paul and Daisy Soros Foundation.

Contents

Chapter 3

List of Figures

List of Tables

Chapter 1

Tools for the study of single molecules: Optical Trapping and Force Clamping

1.1 Introduction

Molecular motors play an important role in driving some of the most complex and important tasks in biological systems, ranging from transcribing RNA from a DNA template (Polymerases) to muscle contraction (Myosin) and propelling bacteria (Flagellum). Among the most well characterized molecular motors are those that move through cytoskeletal fibers such as actin and microtubules. Myosin motor, for instance, is a motor that interacts with acting filaments, whereas dynein and kinesin interact with microtubules. A vast majority of cytoskeletal motors, in general, share a common design theme: they possess a catalytic motor domain with binding sites that allow simultaneous binding to an ATP molecule and a filament track. As such, these motors have the remarkable ability to transduce chemical energy into useful mechanical motion and force generation (and do work). Key to the understanding of the fundamental principles and designs by which molecular motor function

has been the kinesin family. The goal of this thesis is to present recent efforts in the Lang Laboratory to develop tools to study molecular motors, with special emphasis on elucidating the biomechanical mechanisms by which Kinesin generates force and moves. We present recent developments that allow us to force clamp kinesin, preliminary designs of novel kinesin mutants, and study the kinesin - -e-hook interaction using rationally laboratory designed peptides. We further propose new experiments and present specific aims to guide the expansion of the work presented in this thesis.

Over the last decade, advances in optics and electronics have led to the development of an arsenal of tool capable of studying molecules and substrates at the single-molecule level. Techniques such as optical trapping, magnetic tweezers and atomic force microscopy (AFM) have opened new areas of research and an increased interest in the role of forces from the atomistic to the systems level in biological organisms. In fact, so much has been learned about the importance of forces in health and disease, that it has been proposed that research efforts in biomechanics also include the "sequencing" of the Mechanome [7], described as a systems-level view of the role of forces, mechanics, and machinery in biological systems. Ultimately, one can imagine that just as the sequencing of the genome has led to an even greater understanding of disease states, so will elucidating the mechanome. While unraveling the secrets of the mechanome may take a few years, the tools used today will greatly contribute to putting these pieces together.

1.2 Optical Trapping

While magnetic tweezers and atomic force microscopy have been successfully used in force spectroscopy experiments[8], optical trapping stands as versatile tool that can be applied in many different scenarios (See Table 1 for a comparison between each technique).

Optical trapping allows for up to 100pN forces be exerted on particles ranging from polystyrene beads in the ~ nm range to whole cells. Optical traps also have high refresh rates and can dynamically be used to move or track particles in a microscope slide, thus making them perfect tools to non-invasively study the effects of forces and motion in 3-dimensions. In the past 10 years, optical traps have been successfully used to unlock some of the most fascinating details of how molecular motor work. For instance, the use of optical traps allowed the direct measurement of kinesin moving along microtubules under varying conditions and eventually led to the important conclusion that kinesin hydrolyses one ATP per 8-nm step [9].

	Optical tweezers	Magnetic (electromagnetic) tweezers	AFM
Spatial resolution (nm)	0.1–2	5–10 (2–10)	0.5–1
Temporal resolution (s)	10^{-4}	10^{-1}–10^{-2} (10^{-4})	10^{-3}
Stiffness (pN nm^{-1})	0.005–1	10^{-3}–10^{-6} (10^{-4})	10–10^{5}
Force range (pN)	0.1–100	10^{-3}–10^{2} (0.01–10^{4})	10–10^{4}
Displacement range (nm)	0.1–10^{5}	5 –10^{4} (5–10^{5})	0.5–10^{4}
Probe size (μm)	0.25–5	0.5–5	100–250
Typical applications	3D manipulation Tethered assay Interaction assay	Tethered assay DNA topology (3D manipulation)	High-force pulling and interaction assays
Features	Low-noise and low-drift dumbbell geometry	Force clamp Bead rotation Specific interactions	High-resolution imaging
Limitations	Photodamage Sample heating Nonspecific	No manipulation (Force hysteresis)	Large high-stiffness probe Large minimal force Nonspecific

Table 1: Comparison of the most popular techniques used to study single molecules. Table adapted from [8].

A trapped object in the Rayleigh regime, where the object is much smaller than the wavelength of light, can be treated as a dipole. With this approximation, optical forces can be split into two components: a scattering component in the direction of light propagation

and a gradient component in the direction of the intensity gradient of light [10]. In terms of momentum conservation, the force acting on the bead results from a change in the momentum of incident rays diffracted as they pass through the bead and this in turn produces a restoring force that keeps the bead in place (See Figure 1). An additional consideration when designing an optical trap is to use infrared radiation in order to reduce optical damage. A high numerical aperture (NA) objective is also preferred as it allows for a greater trapping efficiency and low power loss.

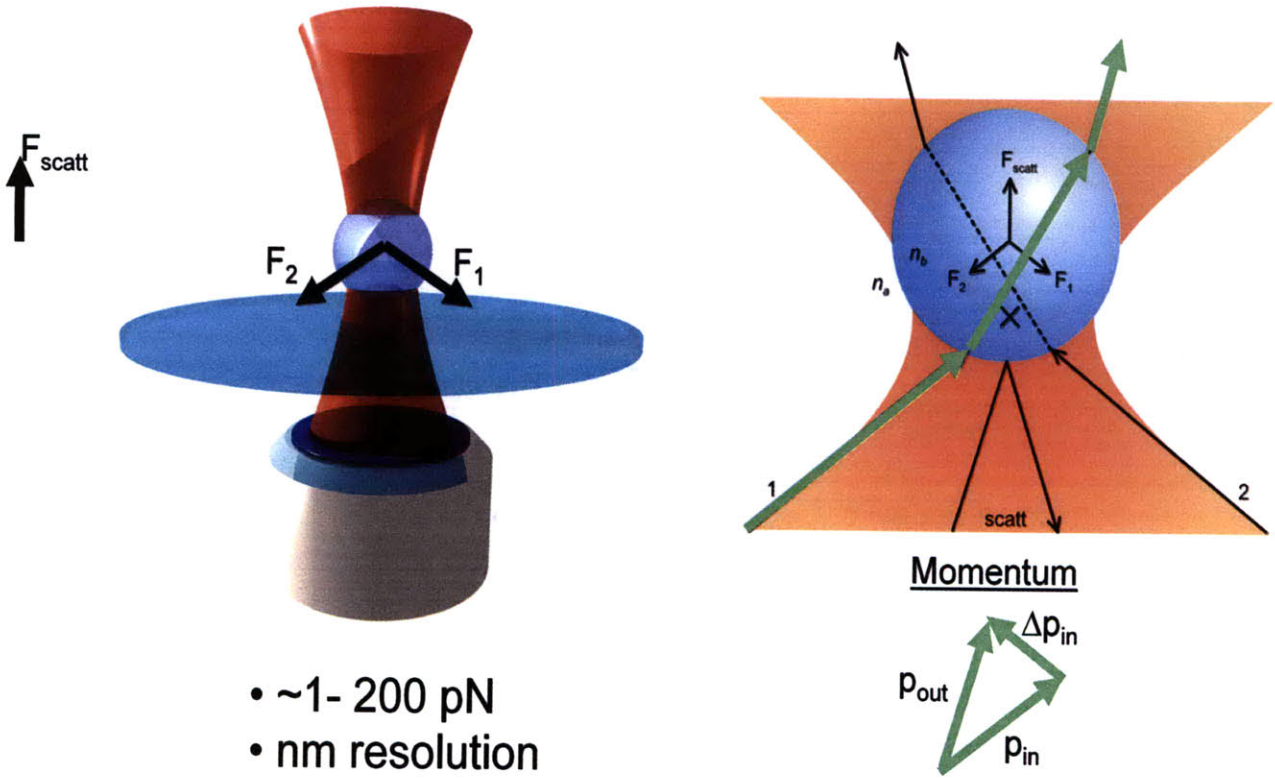

Figure 1: The change in momentum of incident beams causes a net restoring force that serves to keep the bead in place. Forces of up to 100pN can be generated this way. Two components can be used to describe the forces on the bead: a gradient force component moves the bead into the center of the trap and a scattering component pushes it along the direction of light propagation.

The design of an optical trap is straight forward but a few considerations should be taken into account. The basic required elements for a fully functional optical trapping setup are: a trapping laser, steering optics and shutters, a high NA objective, a sample holder and a camera. In addition, it is also convenient to use a stable inverted microscope that can accept multiple light sources is ideal as it can conveniently allow for both trapping laser and fluorescent excitation experiments to be carried out. Also, an appropriate selection of laser wavelength is required to prevent biological damage or heating. In our setup in the Lang Laboratory, a 1064nm laser is used to trap and an additional 975nm laser used as a detector. Control of the trap, including its stiffness, can be added by introducing additional components into the setup. These components can include amplitude modulating elements (such as a polarizer) as well as an Acoustic-Opto Deflector (AOD) to specifically control the optical beam. A high precision stage (such as a piezoelectric stage) with minimal backslash is also an important element to consider when experiments require the use of force clamping techniques. A position detector is also an important consideration for the device. Detectors such as a Position Sending Module (DL100-7PCBA, Pacific Silicon Sensor Inc.) can be used to track the centroid of the intensity pattern of light as it is disturbed by the trapped bead. The incorporation of a second laser beam (a detector beam) can be used to calibrate the trap, a procedure described in the next section. A full schematic of the trapping setup in the Lang Laboratory is presented in Figure 2.

The trapping laser is arguably one of the most critical components of any optical trapping device. It must be able to deliver a single mode output, a Gaussian TEM00 mode, with great stability and minimal power fluctuations. Any changes in the stability of the laser could be reflected as unwanted displacements of the trap and any corrections can introduce noise and reduce the power output. Loss of power output is undesirable, as it can decrease

the trapping force. In general, the trapping force is of the order of 1pN per 10mW of power delivered [11]. For the experiments later presented in this thesis, forces of the range of 5pN, the stall force for kinesin, were used. Another important consideration is the wavelength to employ while working with biological samples. Typical wavelengths in the IR rage (~750-1200 nm) are employed in trapping experiments. Given these requirements, the typical laser of choice is the neodymium:yttrium-aluminum-garnet (Nd:YAG) laser.

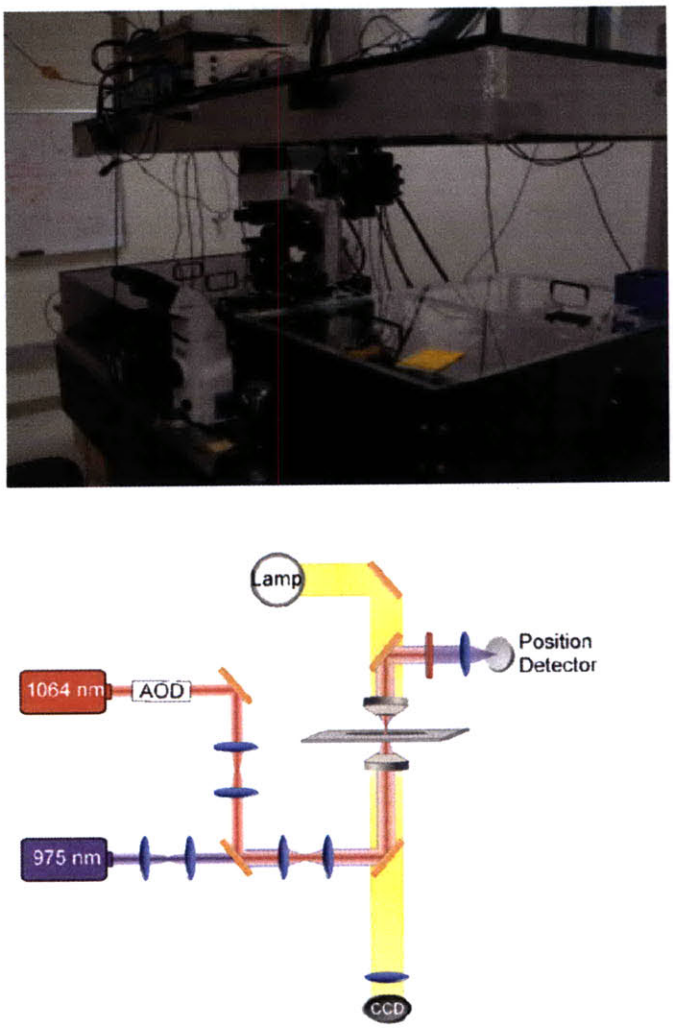

Figure 2: Lang lab laser setup. The top picture shows the inverted microscope with the enclosure housing the optics to the right. The bottom picture shows a diagram of the laser setup. A 1064nm laser is used to trap and a 975nm laser used as a detector.

1.3 Displacement Detection

The detection of position and displacement for objects trapped with an optical trap can be a difficult task. Thermal motion, typically in the order of kT ~ 4pn-nm, can make it a difficult task to discern noise from actual motion, making the use of a trap an important tool when studying processes at the nanometer scale. For instance, the motion of kinesin walking along a microtubule or the transcriptional progress of a tagged RNA polymerise (RNAP) over the length of DNA [12] can be observed and measured with the aid of an optical trap. Currently, position tracking is usually achievedin two ways: using a Video base position detection setup or a back focal plane position detection setup.

1.3.1 Video based imaging position detection

A video camera mounted to the microscope can be used to directly keep track of an object such a polystyrene bead. The system must first be calibrated by matching a pixel to an actual length or distance standard using a ruled micrometer or a commercially available and already calibrated piezoelectric stage. The next step is to find the bead centroid using computational algorithms and edge detection techniques [13]. This setup is mainly limited by the video acquisition rate and the amount of memory that can be stored by the computer system. Figure 3 shows a bead bound to polymerized microtubules under bright field illumination. Current bright field cameras can easily visualize the bead motion over the microtubule for an entire field of view.

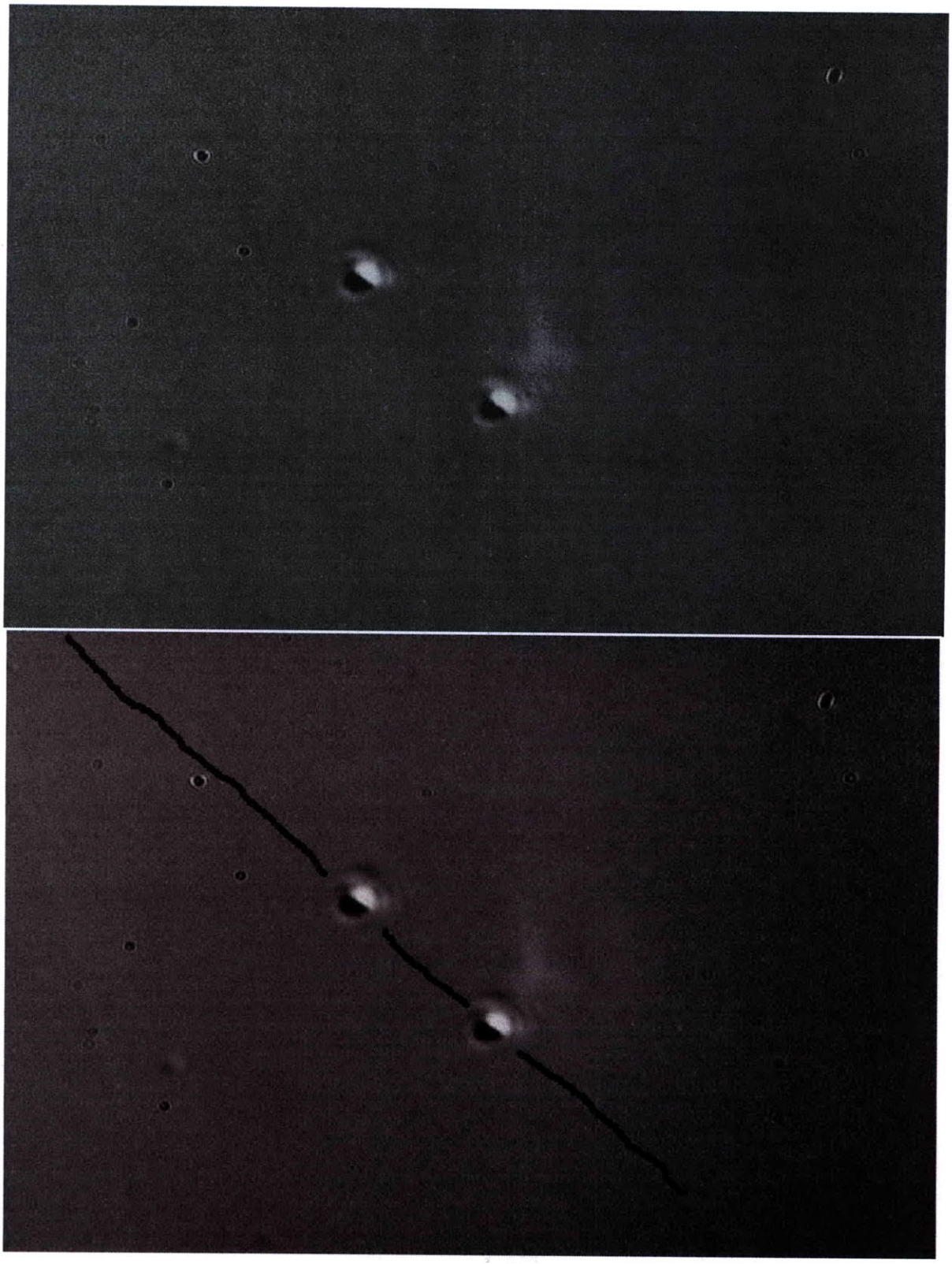

Figure 3: The top figure shows a raw image acquired on the microscope. The bottom image highlights (in black) the faint outline of a microtubule.

1.3.2 Back focal plane displacement detection

Another approach to determining the two-dimensional position and displacement of an object under the microscope (e.g bead) is by using a quadrant photodiode (QPD) placed in the back focal plane of the microscope lens. Simply put, as the detection laser is scattered by the bead, an intensity pattern is formed in the back focal plane (Figure 4 illustrate this method). The formed intensity pattern represents the angular intensity distribution of light that has passed through the focal plane. The intensity pattern has a centroid that can be detected using a QPD. The QPD, shown in Figure 5, is made up of four independent photo diodes that generate an electric current proportional to the intensity of the incident light. The signals from each QPD quadrant are summed pairwise to generate x and y positions. An example of a commercially available position sensing module is shown in Figure 6.

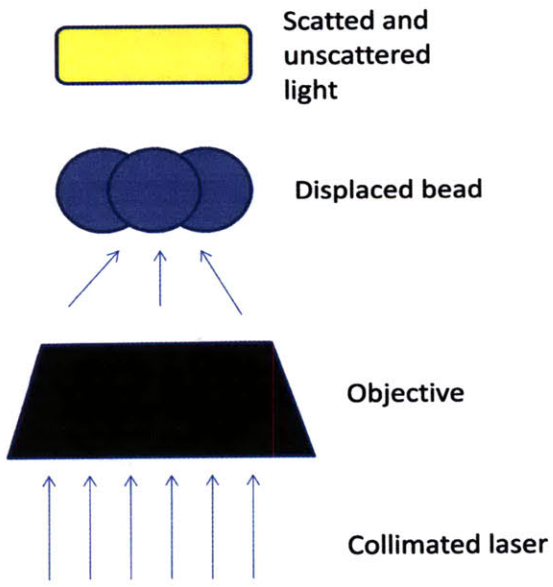

Figure 4: Back-focal-plane displacement detection setup. A collimated beam is tightly focused on the bead and the scatter collected.

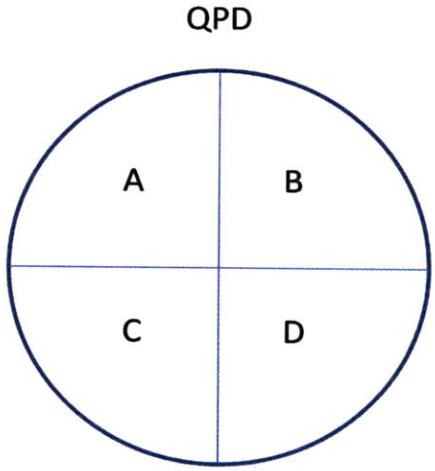

Figure 5: Schematic diagram of a quadratic photodiode (QPD). The signals from each diode quadrant are summed pairwise, and differential signals obtained for X and Y coordinates.

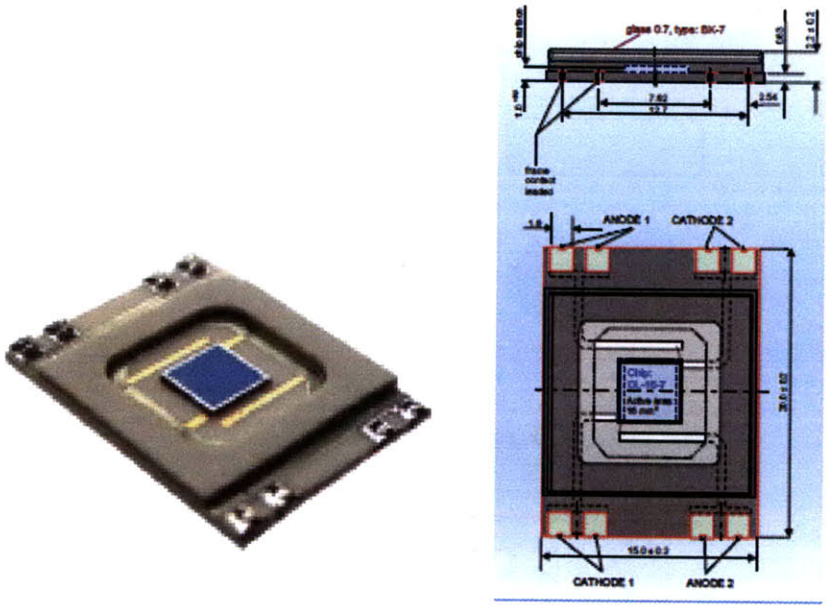

Figure 6: Position sensing module (Pacific Silicon Sensor Inc.) Similar to the QPD in performance but does not use the 4 Quadrant method

1.4 Trap Calibration: Theory

Optical traps allow for the precise measurement of forces and displacements. The first step to determine displacement and forces is to precisely calibrate the trap. Three important calibration procedures can be used to determine trap stiffness: Stokes drag, equipartition theory, and power spectrum. For position and displacements, one can rely on the use of video cameras or QPD sensors by matching position to a measured voltage as previously described. In the Lang laboratory, the calibrating procedure is controlled by a computer and requires the use of an Acousto-Opto deflector to precisely sweep the laser beam while collecting a signal through the QPD. Two types of calibrations are important: those to determine position and those that calibrate for trap stiffness in order to measure forces.

1.4.1 Position Calibration

Methods to determine bead position are described in detail in the literature [2]. In this approach, a one-time video calibration of the AOD against known positions in a stage is made in order to verify proper AOD positioning. This calibration, in addition, will allow the conversion of AOD frequency space (in MHz) to position (in nm) space. In our setup, the conversion factors used to determine position in the X axis is 1148.1nm/Mhz and Y axis is 1041.1 nm/Mhz. Position calibration is a crucial step as it is necessary for the Stokes drag and Equipartition stiffness calibration methods.

As preciously described, a video camera mounted on the microscope can be used to determine position and displacement of an object. Two other methods for determining position and position calibration exist and make use of the QPD, thus making them faster

and more reliable. The first method scans a sample object (eg. Bead) through a grid of known displacements (using an AOD or a piezoelectric stage) and measures the voltage response of the QPD as illustrated in Figure 7. Voltages are then converted to actual physical space using a 5th order 2D polynomial (See Appendix B, ConvertVtoNM.m) A limitation of this method is that measurements are limited to those points where position as a function of voltage is single valued, an area that is approximately 200 nm in the Lang lab setup.

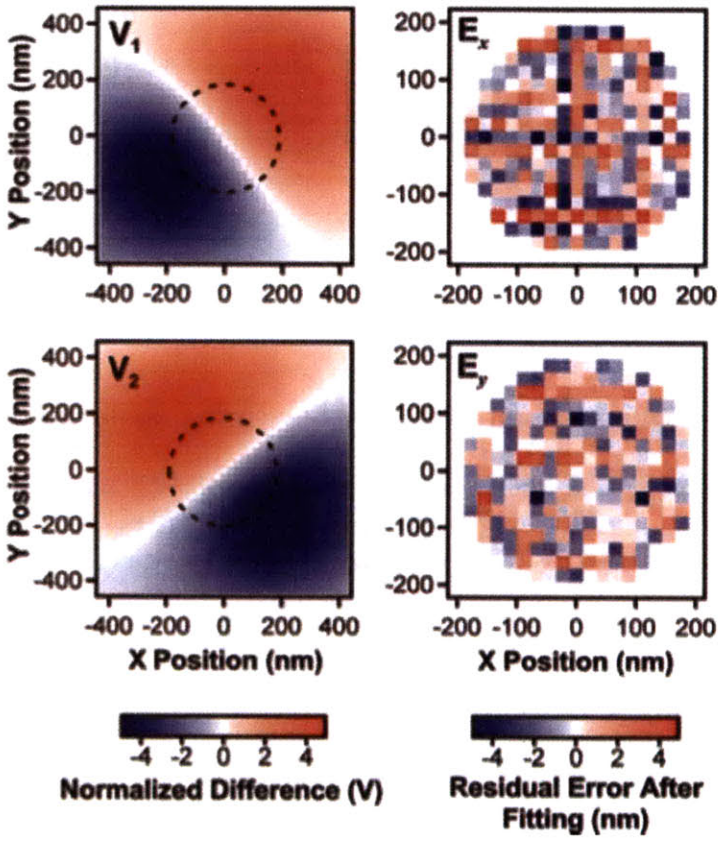

Figure 7: 2D calibration of the QPD. Voltage on the QPD is measured as a bead is moved over a grid of points using an AOD or a stage. This figure shows a grid of 41x41 with ~20 nm spacing in order to demonstrate the detector response. The bead is held at each grid position in the detector, the QPD response measured and converted to position. The QPD can only be used in the circular region outlined, where the voltage as a function of bead position is singled valued. Figure from [2].

To map voltages into x-y spatial coordinates, two fifth order linear least squares fits are required:

$$X(V_1, V_2) = \sum_{i,j=0}^{5} a_{ij} V_1^i V_2^j \text{ and } Y(V_1, V_2) = \sum_{i,j=0}^{5} b_{ij} V_1^i V_2^j$$

In practice, we use 5th order polynomial as a good approximation that makes it computationally efficient to match QPD voltage to position using Labview. Figure 8 shows the Labiew VI used in the Lang laboratory to perform calibrations.

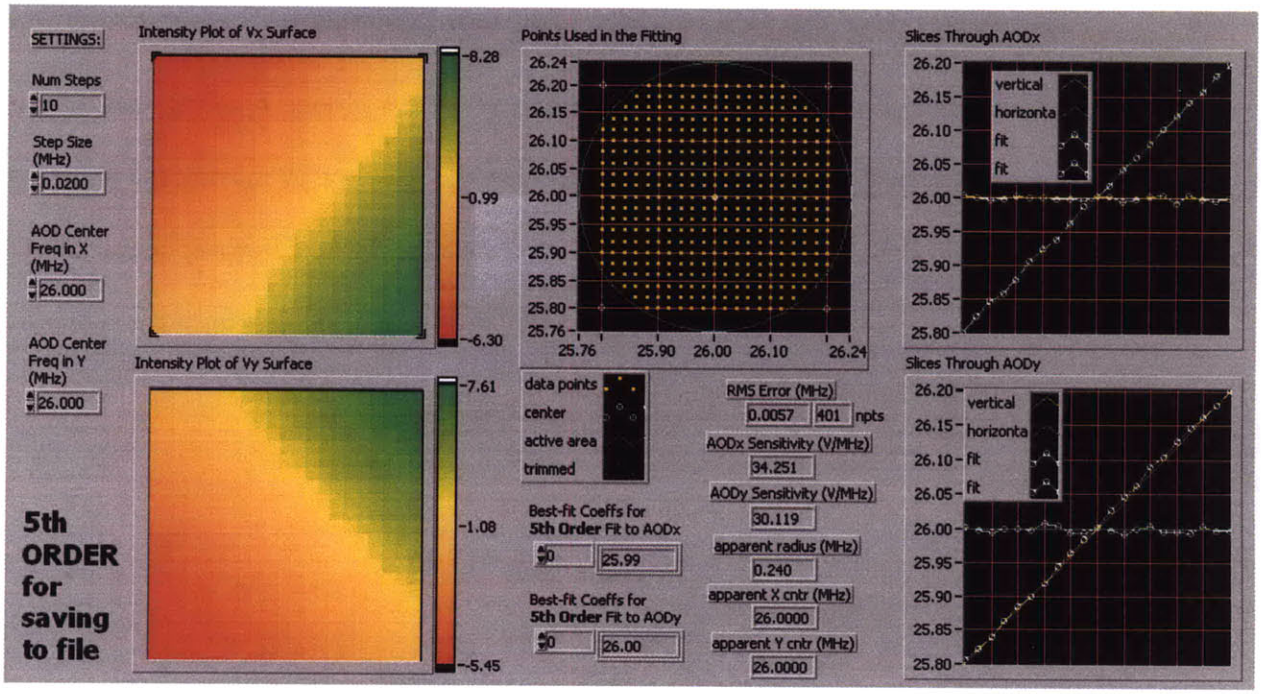

Figure 8: Labview control panel demonstrating the calibration process. A bead is scanned through the detector and the PSD response measured. Then, a 5th order polynomial used to map voltage to x-y coordinates. The circular region shown in the figure represents the ~200nm area used to detect bead position.

1.4.2 Stiffness Calibration

Properly calibrating the stiffness of the trap is an important step before starting each experiment as instrument drifting and power variations can adversely affect the amount of measured force. Three methods can be used in order to calibrate the stiffness of the trap: Stoke's drag, equipartition, and power spectrum.

Stokes drag

The Strokes drag method for calculating the stiffness of the trap takes advantage of the fact that for small displacements, the trap behaves like a Hookean spring. Basically, a displacement is applied to a trapped bead using either the AOD or by moving the stage. As the bead moves, a drag force opposes the applied translational force. For a spherical object moving at a velocity v, in a media of density η, and displaced a distance x from the center of the trap, Stokes law can then be used to calculate the trap stiffness k:

$$F_{Trap=}F_{drag}$$

$$kx = 6\pi r\eta v$$

Equipartition

Another way to calculate the stiffness of the trap is by using the equipartition theorem. The equipartition theorem states that for a Harmonic energy landscape each degree

of freedom contains ½ kT of energy. In the case of an optical trap modeled as a Harmonic oscillator, one can show that:

$$\frac{1}{2}k_B T = \frac{1}{2}k\langle(x - x_{mean})^2\rangle$$

This expression reduces the problem of finding the stiffness of the trap to that of experimentally determining the variance of position fluctuations and relating that to the equipartition theorem. It is convenient to point out that this method does not rely on parameters such the medium density, velocity or particle size. Figure 9 summarizes the outlines trap stiffness calibration methods.

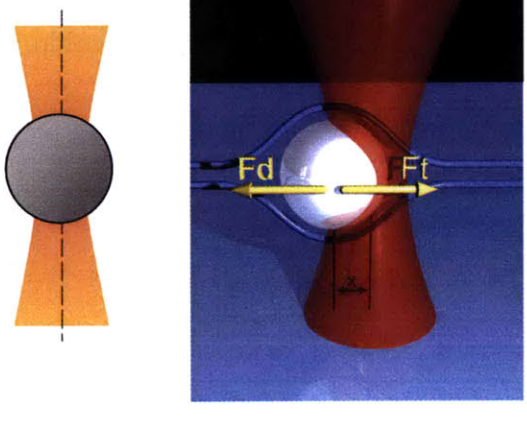

Trap stiffness calibrations

1. Brownian motion: Variance in bead position is an indicator of trap stiffness

$$\frac{1}{2}k_B T = \frac{1}{2}k_{trap}\left\langle x^2 \right\rangle$$

2. Stokes Drag: Measure bead displacement when subjected to known drag force

$$F = 6\pi\eta r v = k_{trap} x$$

Figure 9: Methods to calibrate the optical trap.

Power Spectrum

Yet another way to calculate the stiffness of an optical trap using the QPD is by recording the Brownian motion of a trapped bead and then calculating its power spectrum. This method is based on the fact the power spectrum of a trapped bead can be described by a Lorentzian [14] such as the one shown in Figure 10. In one dimension, the power spectrum is given by:

$$S_x(f) = \frac{k_B T}{\gamma \pi^2 (f_c^{\,2} + f^2)}$$

Sx(f) is the power spectrum of the position x(t) of a spring with constant k and f_c is the characteristic frequency of the trap or corner frequency, defined as $f_c = k/2\pi\gamma$. Another important parameter is $S_0 = \frac{4\gamma k_B T}{k^2}$ at frequency f << f0, which reflects the confinement of the particle. The stiffness k can then be determined from the relationship:

$$k = \frac{2k_B T}{\pi S_0 f_C}$$

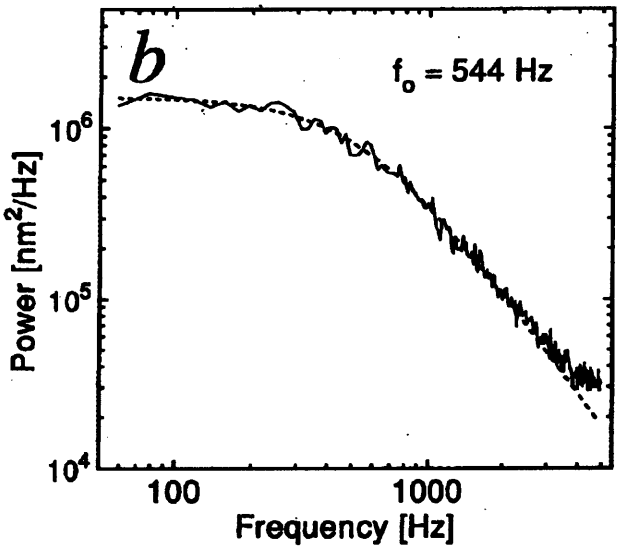

Figure 10: Thermal noise spectrum of a trapped silica bead held by an optical trap. Solid line represents a Lorentzian fit. The corner frequency is 544 Hz and the trap stiffness k = 1.9x10E-2 pN/nm. Figure adapted from [3].

Note on the trap linearity

It is important to point out that the key approximation that allows for an easy calculation of the trap stiffness is the linearity of the trap for small displacements as shown in Figure 11. Approximating the trap as a harmonic potential allows for the trapping laser to act as a Hookean spring with spring constant k in the range of about ~ 200nm. A complete form of the force acting on the bead is available in the literature [15].

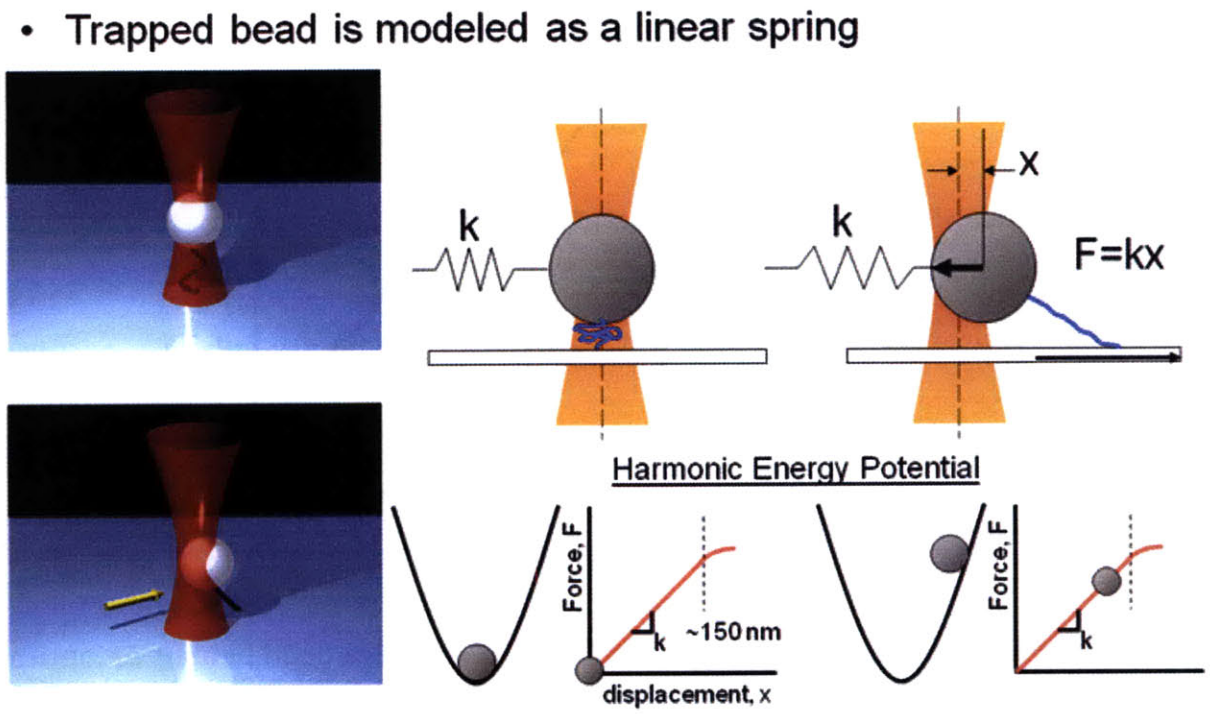

Figure 11: For small displacements, the optical trap behaves like a Hookean spring. Figure from Carlos Castro.

1.5 Force Clamping

Optical traps have been successfully used to study molecular motors such as kinesin and RNA polymerase [12, 16]. Early traps were stationary and thus unable to exert constant forces without the help of a manual operator moving the microscope stage. The development of QPD and AOD devices has allowed the precise tracking of bead motion with nanometer accuracy and high bandwidth while precisely steering the trapping beam. A significant advantage of combining QPD and AOD devices in an optical trap is that they allow for experiments to be automated and offer added repeatability.

Computer controlled traps also allow for two experimental conditions: Position clamping and Force clamping. In the position clamping configuration, the trap light intensity or its location is adjusted to keep the bead at a fix position, thus allowing for motor stall forces to be determined. Force clamping, on the other hand, requires that the trap intensity or location be varied in order to apply a constant load. Fore clamping is particularly useful when studying molecular motors as it allows for longer runs (clearer processivity measurements) and reduces noise introduced by Brownian motion. For instance, a force clamp can be used to directly observe the steps of kinesin moving along a microtubule as shown in Figure 12. More importantly, force clamping allows the study of molecular motors under constant and reproducible conditions.

Proteins such as kinesin undergo chemical and mechanical transitions such as substrate binding, unbinding, and ATP hydrolysis that occur at multiple sites in the protein. The rate of these transitions may as well be affected by the direction and magnitude of applied forces [16]. Understanding how these rates vary with force and direction will ultimately provide us with valuable insights into how molecular motors function and what models can be best used to describe them.

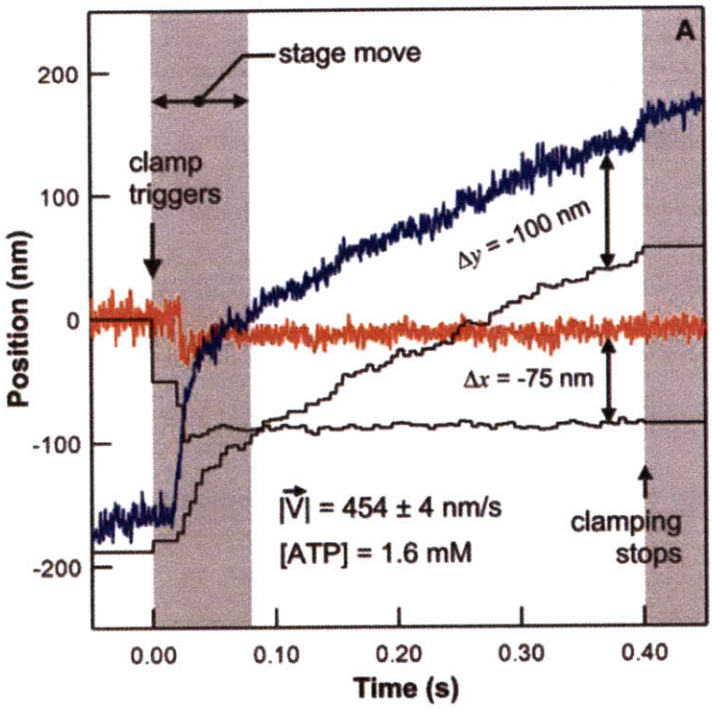

Figure 12: Force clamp in action. Kinesin powered bead movement is shown in red for the X axis and blue for the x. The optical trap displacement is shown in black. Figure adapted from [2].

Force clamping is an important tool to study kinesin as it allows for long records of kinesin walking on microtubules at a constant force (less than the 5 pN stall force) and the study of rate limiting steps in the kinesin cycle as previously done by Lang et al.

1.5.1 Force Clamp Design and Testing

A great amount of effort was spent in designing and testing a force clamp that can be used for the study of kinesin in the Lang Laboratory. To meet the laboratory requirements, the force clamp would need to be able to track the position of a bead with a tagged kinesin

moving along a microtubule. For simplicity, we implemented a 1-D force clamp in Labview using an AOD to steer the trapping beam. Shown in Figure 13 is the user interface of the force clamp and shown in Figure 14 is an illustration presenting the basic function of a force clamp. The implemented Labview program was able to keep track of the average bead position and then, once placed over a microtubule, allowed the bead to be displaced from the middle of the trap a pre-determined distance. In most of the experiments performed (and in an ideal setup), we setup the clamp so that for a distance of ~ 100 nm between the trap and the bead, and a stiffness of 0.05pN/nm, the corresponding force would be 5 pN, the stall force of kinesin.

Running the force clamp requires a combination of steps:

1) The bead needs to be calibrated in order to determine its position. This step is automated and the signal is filtered at 30 kHz.

2) Once calibrated, the bead is placed on top of a microtubule. This step is currently done manually, but a module for controlling a piezoelectric stage can be easily integrated in the future.

3) The force clamp parameters are setup, including the force direction and distance between the bead and the center of the trap. The force clamp is started and the acquisition filter set to 2 kHz so as to obtain a clean signal.

4) The bead motion is monitored and manual adjustments performed. It is sometimes necessary to manually reset the trap.

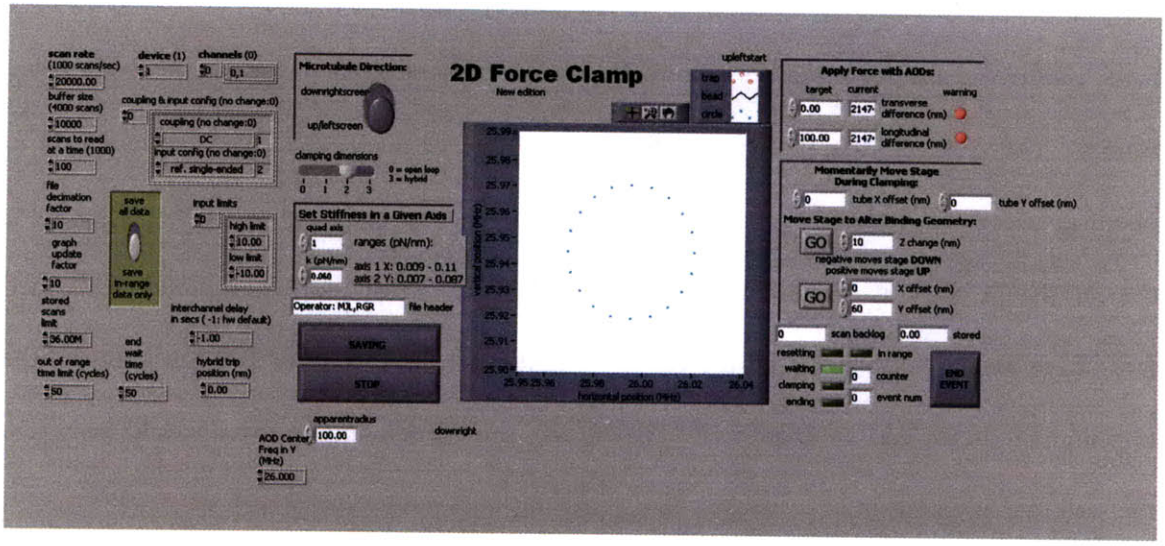

Figure 13: Labview VI showing the user interface for the 2D clamp developed in the Lang lab.

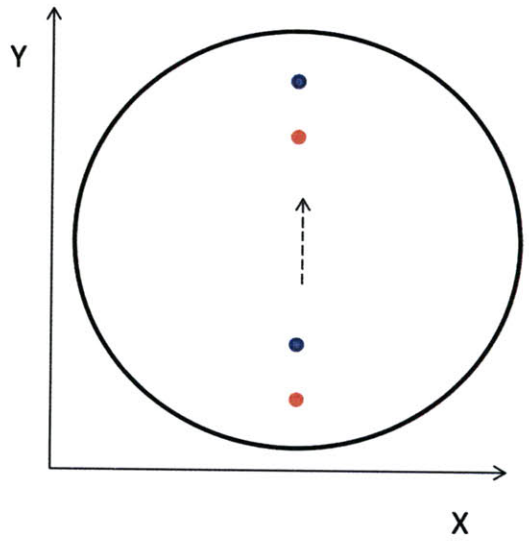

Figure 14: Principle behind the force clamp. The blue dot represented a bead with kinesin, and trailing behind in red is the optical trap. The distance between both points is linearly related to the force (F = kx). The circle is the area ~200nm calibrated to determined bead position. As the bead moves, the trap center follows.

1.5.2 Results

With the current setup, the force clamp was shown to work quite successfully. Later we show the performance of the trap when following kinesin. Shown in Figure 15, Figure 16, and Figure 17 are sample traces demonstrating the force clamp in action. Notice that in the case of Figure 15, the trap was setup to hold at a distance of ~30 nm. From the collected data, the trap was in fact able to keep a mean distance of 27.34 nm with a standard deviation of 1.33 nm. The small difference between the desired distance and the actual measurement can be traced to perhaps a lag between the bead detection and the subsequent command to steer the laser.

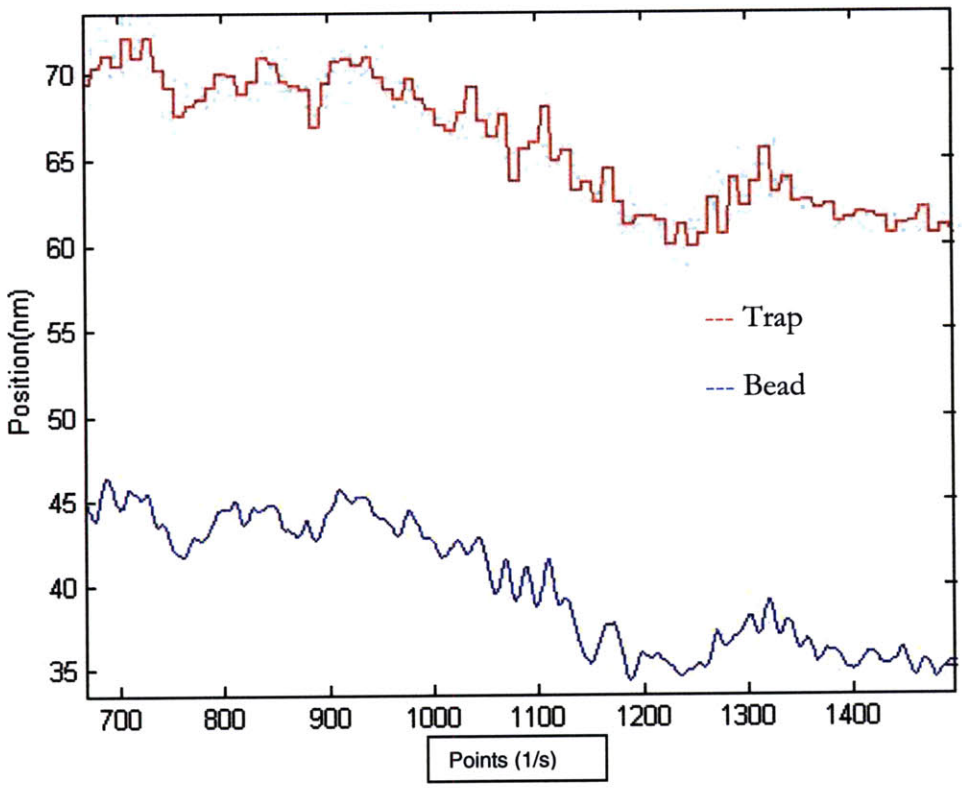

Figure 15: Sample Force Clamp. Average distance set up 30 nm.

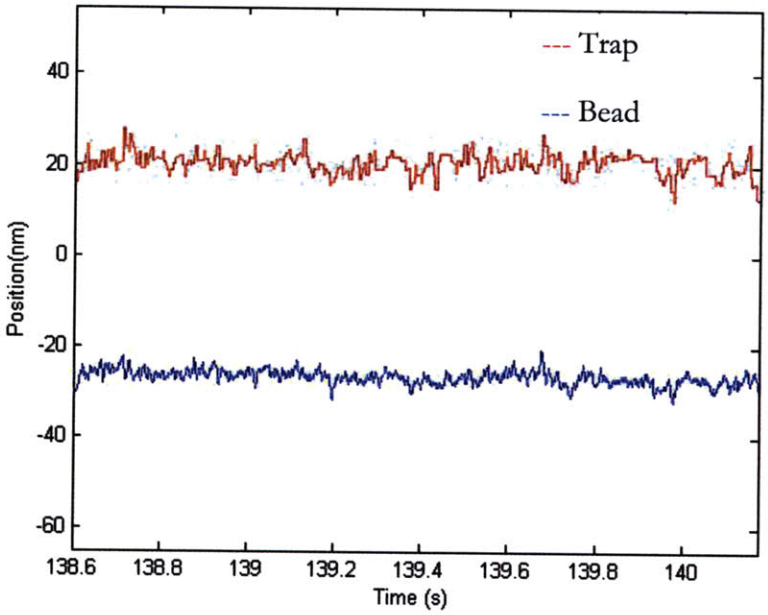

Figure 16: Sample force clamp trace. The trap position in red leads the bead. The spacing was set for ~50 nm.

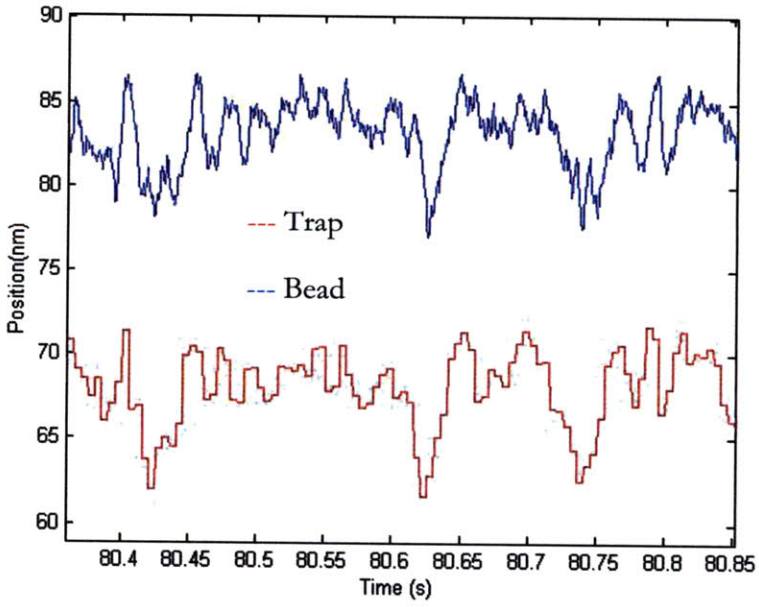

Figure 17: Another sample force clamp trace. In this case, the bead position in blue leads the trap in red. The spacing was set for ~15 nm.

Chapter 2

Kinesin: Mutants, E-hook, and new tools to elucidate the kinesin force generating mechanism.

2.1 Introduction

As a model system, kinesin is well suited for laboratory work. Kinesin is the smallest molecular motor and is also considered the simplest, thus it is prone to easy molecular manipulations and *in vitro* assays. Kinesin has been instrumental in further advancing our understanding of how molecular motors generate force, respond to applied force and move. Advances in instrumentation and molecular manipulations have allowed for the first time a direct measurement of how a single kinesin molecule, attached to a bead, walks along a microtubule track. Ultimately, understanding how kinesin walks and generates force represents a most beautiful task as it requires an elegant interplay between accurate model prediction and experimental validation. In addition, a clear understanding of kinesin and its role in cellular transport could lead to a better understanding of diseases such as Alzheimer's and Huntington's, where transport mechanisms have presumably failed.

2.2 Kinesin: Protein structure and role in disease.

The kinesin family consists of a large number of microtubule proteins capable of converting the free energy of the γ-phosphate bond of ATP it into useful mechanical work in order to direct the movement of cargo in a directed manner along microtubules. There are 14 recognized kinesin families. For the purpose of this thesis, we use as DmK401 – Drosophila kinesin, a member of the kinesin-1 family [17]. The defining characteristic for a kinesin protein is its catalytic core, commonly known as the "motor domain". The motor domain is a highly conserved unit with ATP and microtubule binding sites joined by a less conserved α-helical coiled-coil stalk. The region between the motor domain and the coiled coil is commonly referred to as the neck-linker, a mechanical element that undergoes nucleotide dependent conformational changes. The neck-liner is in turn responsible for the "powerstroke", a conformational change that propels the head forward and determines the directionality (toward the - or the + end of a microtubule) of the motor.

The most widely studied form of kinesin is Kinesin-1, also referred to in the literature as conventional kinesin. Conventional kinesin was the first kinesin motor to be identified and purified from cell extracts [17]. Structurally, conventional kinesin is made up of two monomers and each, in turn, is made up of an N-terminal motor head, a neck linker, a long coiled-coil dimerization region and a globular tail domain. In addition, the active form of conventional kinesin is a dimer with the coiled-coil regions of two monomers wound together to form a 70 nm stalk (See Figure 18).

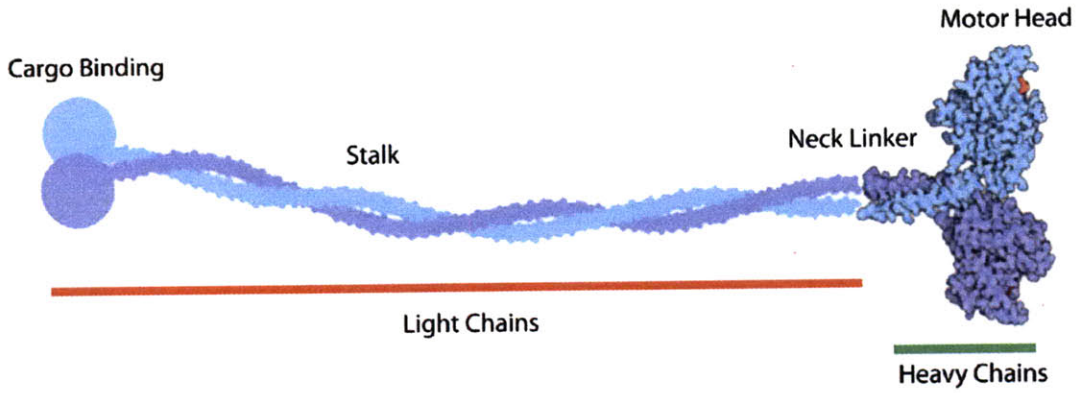

Figure 18: Kinesin structure. Kinesin is made up of two monitors (shown in blue and purple) and several light chain segments twisted around each other. Figure adapted from [4].

Kinesin motor proteins have been linked to devastating diseases characterized by the defective transport of cell components, transport of pathogens, or cell division. Neurodegenerative conditions such as Alzheimer's are characterized by the aggregation of proteins in the neuronal cell body, interruption of axonal transport and eventual axonopathy, states that are simulator to those generated by disrupting kinesin mediated transport. Further evidence indicates that amyloid precursor protein (APP), involved in Alzheimer's disease, directly interacts with kinesin, suggesting a link between APP carriers and a motor. Another protein involved in Alzherimer's disease, protein tau, can directly inhibit motors on microtubule tracks. When combined, these observations suggest that in Alzheimer's disease, kinesin mediated transport play an important role [18].

Kinesin also plays an important role in cancer and the cell cycle. For instance, a variant of kinesin-1, KIF1B, is downregulated in neuroblastomas and could even function as a tumor suppressor [19]. Another variant of kinesin, KF5B, has been identified bound to NF1 and NF2, two neurofibromatosis tumor suppressors[20]. Kinesin is also important for

mitosis and when inhibited can disrupts the cell cycle. For instance, Taxol, a drug commonly used for breast cancer treatment, disrupt cell cycle progression by stabilizing microtubules and disrupting proper kinesin mediated movement during mitosis.

Microtubule dependent transport is required by some viruses in order to move around the cell. Kinesin represents the perfect motor to drive viral cargo around the cell. For instance, in the case of neurotropic herpes viruses, kinesin-dependent transport is essential as these viruses must travel long distances from the cell body to the axon terminal of dorsal root ganglion neurons. Disruption of proper kinesin function is also the hallmark of some viral infections that destroy the microtubule track in order to disrupt kinesin mediated transport. One such case is the HIV Rev protein, which can mimic a type of kinesin that depolymerizes microtubules, thus impairing proper cellular function. Other viruses such as the vaccinia virus, a member of the poxvirus family, also rely on kinesin to transport viral protein and enhance its cell-to-cell capacity to spread [18].

Understanding how kinesin works and moves can potentially offer insights into the universally conserved mechanisms by which motor protein works. Furthermore, understanding how molecular motors move around the cell, in general, is important as it can lead to the discovery of novel treatments in certain viral infections, cancer and neurodegenerative diseases. One could easily imagine, for instance, the development of therapies that specifically inhibit kinesin by some mechanism that relates to its walking conformation or mechanism for force generation.

2.3 Kinesin motion: What is required?

Interest in kinesin has sparked a significant amount of research that has helped elucidate the biophysics and properties of its movement. Kinesin has several interesting properties: it can decide which way to move along a track, it can generate force, and can also move long distances without dissociating, a property known as processivity. Kinesin also must travel long distances relatively fast. For instance, transport of membranous vesicles to the axon would take several year by diffusion alone [21], yet kinesin mediated transport of such vesicles occurs in a manner of minutes. Using a combination of single-molecule studies and assays, it has been determined that kinesin moves 8.2 nm per ATP hydrolyzed[9], the same distance between adjacent tubulins. In addition, kinesin can complete ~100 ATP turnovers and walk about 800 nm/sec while generating a force of about ~6 pN [22].

Work by Schnitzer et al. was fundamental at defining experimentally based constraints on theories of kinesin movement or walking [9]. In their work, Schnitzer et al. set out to determine the coupling ration, defined as the number of ATP molecules hydrolyzed per mechanical advance, for kinesin. Using the technique of optical-trapping interferometry, Schnitzer et al. were able to measure, at subnanometer resolution, the average rate of movement of a kinesin molecule that had been tagged to silica beads and deposited onto immobilized microtubules. This work lead to the conclusion that at near-zero load, kinesin hydrolyses a single ATP molecule per 8-nm advance. These results can be used to place constrains on theoretical models of the way kinesin walks. For instance, models that simultaneously required two ATP molecules were excluded. Furthermore, models in which kinesin hydrolyses multiple ATPs per 8-nm, loose coupling or in which ATP hydrolysis results in movement greater than 8-9nm were equally excluded. On the other hand, models

that remained consistent with experimental observations include those in which the centroid of the molecule is displaced in increments of 8 nm, alternating 16 nm steps by each of the two heads or perhaps sliding along. Other consistent models include those in which each ATP molecule produces a composite of two shorter substeps.

A combination of the constraints set forth by the work of Schnitzer et al. with the observation that kinesin is a highly processive motor led to the formulation of two leading and competing theoretical models describing the way kinesin walks. One such model, and perhaps the most widely accepted in the field, is the Hand-Over-Hand model. In this model, one head of kinesin is bound to a microtubule and enters a weak binding state when the second head becomes strongly bound to the microtubule. Binding of the second head in turn is thought to induce a strain, causing the first head to be released from its bound state. The released head then moves to the next binding site and a cycle repeats as kinesin advances, hydrolyzing one ATP per step. The conformation of kinesin at the beginning of each need is not required to be the same (as postulated in the symmetric hand-over-hand), and an asymmetric hand-over-hand model can be also proposed. An alternate model for how kinesin walks is the inchworm model. In this model, the both kinesin heads proceed along the microtubule with one head dragging the other, in complete contrast to the hand-over-hand model. Inherent to this model is the requirement that the motor domain for each head must differ in function so that one heads always leads while the other lags. In addition, given that an ATP is hydrolyzed for each 8nm step, only the leading head must be capable of hydrolyzing ATP. Current findings favor a Hand-over-hand model for kinesin walking [23].

Models of force generation in molecular motors include the powerstroke model (originally proposed by F. Huxley in 1957) and "ratchet" or diffusion models. In the case of

kinesin, a powerstroke model, analogous to that of myosin, seems to agree with experimental evidence[24]. In the powerstroke model, an "elastic" element in the motor protein interacts with a filament to store mechanical energy that is released in the form of a force leading to motion[25]. Diffusion may also plays a role in kinesin motion and force generation[26], making it unclear which mechanism is favored by kinesin: a powerstroke or a "ratchet", or both. Once thing is clear, however, the processes and conformations by which kinesin is able to convert ATP into mechanical force are not fully understood.

As previously described, a lot has been learned about Kinesin and its motion in the past few years. Missing, however, is a clear understanding of the events that take place at the atomistic level in order for the motor domain to bind to the microtubule, go through an ATP dependent conformational change, generate force and ultimately propel forward. Recent MD simulations [27] have identified the force-generating mechanism in kinesin, the cover-neck bundle, and strongly suggest that the formation of the CNB between the N-terminal cover strand and the C-terminal neck linker of the motor head is responsible for force generation. Further experimental results [1] have concluded that kinesins with mutations in the CNB do generate less force, further confirming the conclusions based on MD computational work [27].

2.4 Kinesin: Mechanochemical cycle and force generation mechanism/CNB.

The kinesin mechanochemical cycle has been the subject of much study [28]. It has been determined that when kinesin moves along the microtubule, there is a state when the

trailing head in the ATP state and the nucleotide-free leading head are both bound to the microtubule. Next, ATP hydrolysis from the trailing reduces its affinity for the microtubule at the same time that a new ATP molecule binds to the leading head. These events cause the forward motion of the neck linker that connects the motor head to the neck helix causing it to dock on the ATP-bound head and positioning the trailing head on the next microtubule binding site, completing one cycle as illustrated in Figure 19 [5].

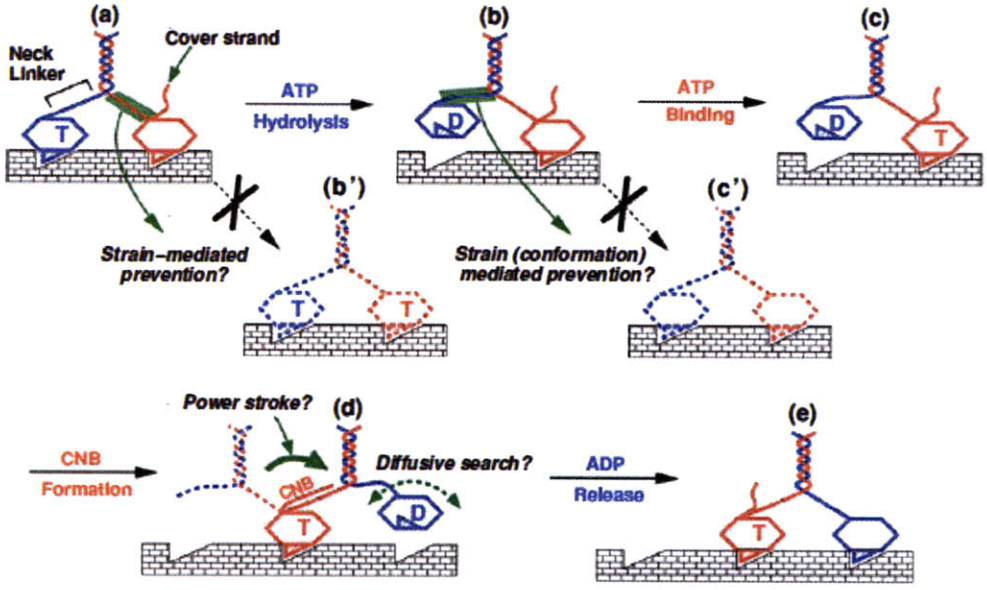

Figure 19: Kinesin mechanochemical cycle . (a) Both kinesin heads with and without ATP have high affinity for the microtubule. It is thought that perhaps a there is a strain-mediated mechanism that prevents an ATP from binding simultaneously both heads as in (b'). (b) ATP hydrolysis on the trailing head reduces its affinity and leads to ADP release. It is thought that state (c') where the trailing head re-binds may be also mediated by mechanical stress. Reduced stain in the neck linker leads to state (c) and CNB formation as down in (d). The newly leading head in blue releases ADP and the cycle repeats (e). Adapted from [5].

While there is plenty of evidence to support the kinesin mechanochemical cycle sequence of events, they are not based on an atomistic understanding of kinesin, but rather

based on phenomenological observation. Central to a complete understanding of kinesin has been the questions, how does kinesin generate force? And what do the different kinesin states look like at an atomic level? Recent work by Hwang et al. [27] has identified a 9 residue domain at the N-terminal end of the kinesin motor head, termed the cover strand, as a key element for force generation. An additional element, a beta sheet between the cover strand and the neck linker, termed the cover-neck bundle (CNB), is an important force-generating element, overcoming loads on the neck stalk and pushing the neck linker forward. This process, a dynamic folding of a domain, is a novel idea and merits further exploration. Furthermore, static crystal structures fail to capture the dynamic nature of the powerstroke and thus may present an incomplete picture.

A complete atomistic and computational model of kinesin will provide new insights into the processes that control motor head coordination (see [29]) and the motion of the unbound head as driven perhaps by mechanical strain, not limited just to a diffusional search argument. Moreover, a refined understanding of kinesin may provide further evidence for more detailed model of kinesin walking.

2.4.1 The Coverneck Bundle (CNB)

The discovery of the CNB formation as an element for force generation in kinesin was no easy task and required a multidisciplinary approach between computational simulations and experimental verification [1, 5]. Available structures and MD simulations were used to predict structures of kinesin that were critical to force generation. Through these simulations, a specific N-terminal segment of kinesin, termed the coverstrand (CS), emerged as a driving element of the force generation mechanism. An additional element, the

neck linker (NL), was shown to combine with the CS to form a β-sheet, the cover-neck bundle (CNB), and together they propel the kinesin stalk forwards to initiate motion.

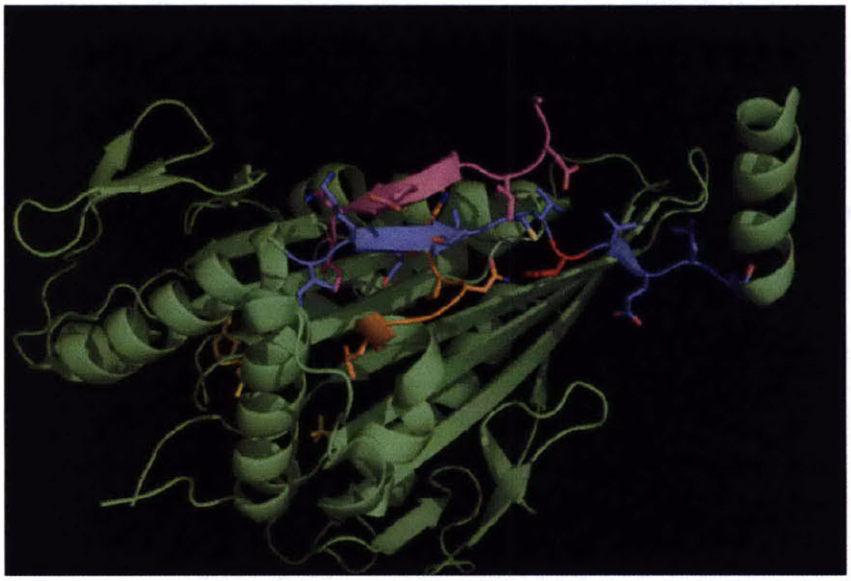

Figure 20: A well formed CNB using 1MKJ PDB, Human kinesin motor domain. In Yellow is an ATP analogue; in Blue the NL; Magenta the CS; Orange L13; and Red Asn latch. Courtesy of Matt Wohlever.

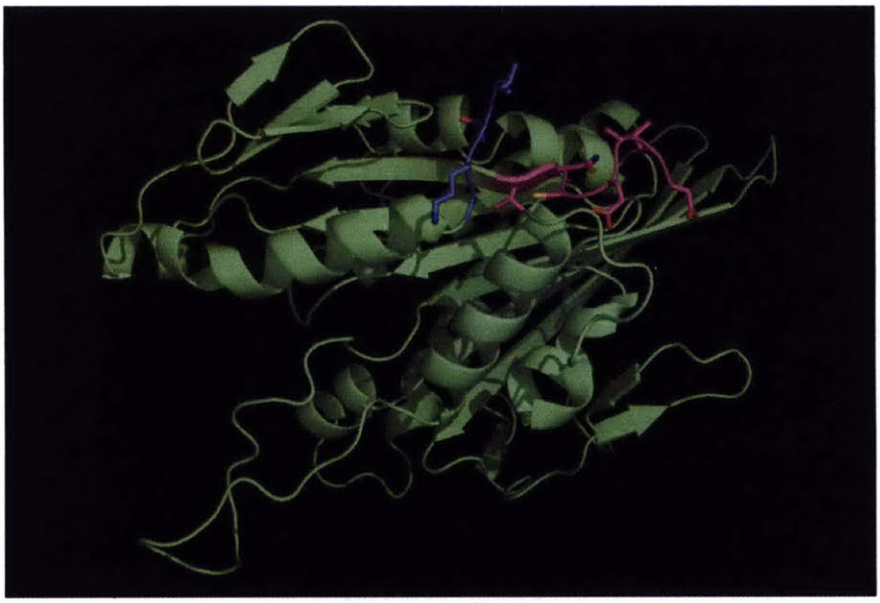

Figure 21: Unordered CNB using 1BG2 PDB, Human ubiquitous kinesin motor domain. ADP bound and NL unbound. Courtesy of Matt Wohlever.

The MD simulations indicate that the stepping cycle and powerstroke for kinesin occurs as follow (see Figure 22):

1) Initially, the CS is not bound to the NL and the leading motor head is in the nucleotide-free state yet bound to the microtubule. CS and NL binding is restricted to α4 (corresponding to myosin's relay helix), which restricts α6 from forming an extra helical turn at the N-terminal base of the NL and keeping the NL out-of-sync with the CS.
2) ATP then binds to the leading head, resulting in the extra turn followed by alignment and formation of the CNB and subsequent powerstroke that propels the trailing head forward.
3) The new leading head then actively searches for the next microtubule binding site or remains weakly bound in a mobile state until ADP release.

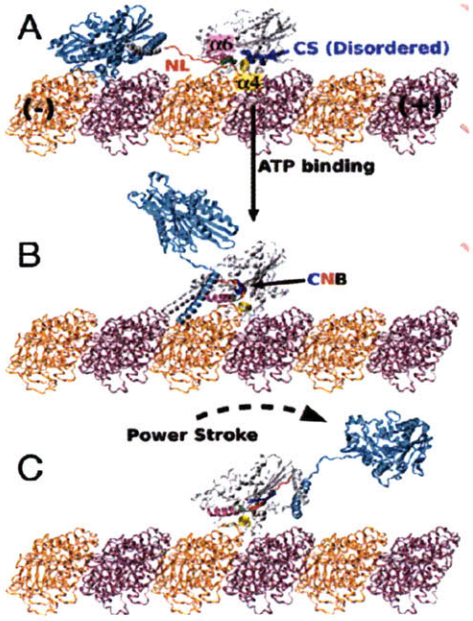

Figure 22: Model of the kinesin power stroke. A) Before ATP binding, the CS and NL are out-of-register. B) ATP binding leads to the formation of the CNB which leads to the powestroke shown in C) and subsequent search for a binding site.

Furthermore, the identification of the CNB as a key element for the generation of force in kinesin offers not only a mechanistic understanding of the inner works of molecular motors in general as many of the common elements of the CNB are conserved as shown in Table 2, but opens up new possibilities for the rational design and engineering of molecular motors with exact specifications.

SwissProt ID	Organism					1		3		5		7		9
(2KIN)	Rat	-	-	-	-	M	A	D	P	A	E	C	S	I
(1MKJ)	Human	-	-	-	-	M	A	D	L	A	E	C	N	I
P28738	Mouse	-	-	-	-	M	A	D	P	A	E	C	S	I
Q6V1L4	Quail	-	-	-	-	M	A	D	P	T	E	C	S	I
Q504B9	Zebrafish	-	-	-	M	T	D	A	A	A	E	C	N	I
Q4S807	Puffer	-	-	-	M	A	D	V	P	A	E	C	N	I
Q3MHM9	Bovine	-	-	-	-	M	A	D	P	A	E	C	N	I
P35978	Sea urchin	-	-	-	-	M	A	D	P	A	E	C	N	I
Q5R9K7	Orangutan	-	-	-	M	A	E	T	N	N	E	C	S	I
P21613	Squid	-	-	-	-	M	D	V	A	S	E	C	N	I
P17210	Drosophila	M	S	A	E	R	E	I	P	A	E	D	S	I
(1I6I; KIF1A)	Mouse	-	-	-	-	-	-	-	M	A	G	A	S	V
(1Q0B; EG5)	Human	S	S	A	K	K	K	E	E	K	G	K	N	I

Table 2: BLAST search outlining conserved in the CS element of the Kinesin-1 family. Adapted from [27].

2.5 Kinesin Mutants

To verify the function of the CNB as predicted by the MD simulations, mutations of the WT kinesin coverstrand sequence MSAEREIPAEDSI were made by Khalil et al. The authors hypothesized that if CNB formation is required for powerstroke initiation in kinesin, a local disruption of the NL and CS could interfere with the ability of the protein to generate force and move forward. Two CS mutants were designed, one with a flexible CS (2G Mutant) by mutating two residues into glycine and another mutant without the CS (DEL Mutant). Figure 23 shows an illustration of the mutants and an SDS page confirming their difference in size. Using an optical trap and custom written MATLAB software, it was

determined that the CS mutants generate less force than kinesin wild-type (WT). Figure 24,A shows stall force distributions, which a shift to the left for the case of the kinesin mutants. Furthermore, and as a consequence of the mutations to the CS, the kinesin mutants showed remarkably altered motile properties such as reduced processivity and load-dependent kinetic steps and increased loaded speeds.

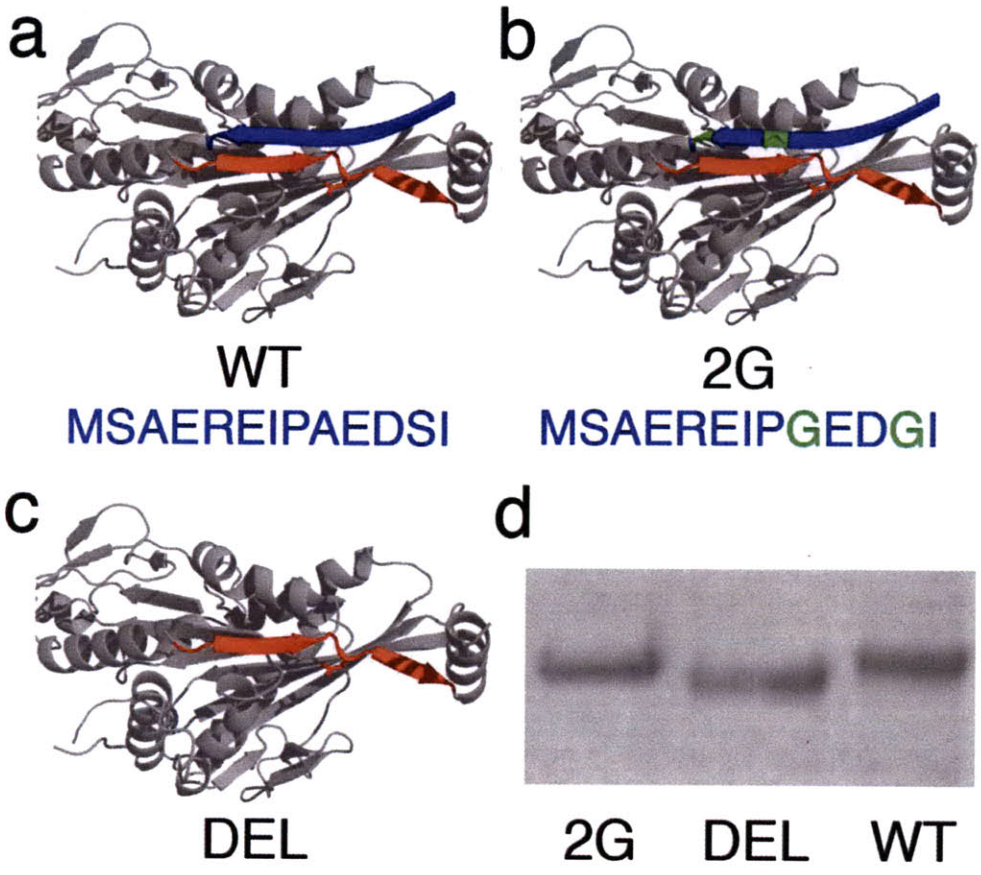

Figure 23: Kinesin mutants. A) Shows wild type, B) shows 2G mutant and C) Deletion mutant. In blue is the full CS ribbon, mutated residues in green and the NL in red. Structures based on 2KIN PDB. D) Shows an SDS page confirming a difference in sizes. Figure from [1].

To quantitatively compare the 2 mutants with WT kinesin, Khalil et al. used an optical trap to determine stall forces (Fs) and force-velocity curves for all 3 kinesin motors. It was found that the mean stall force of mutant 2G was 61% of WT, whereas the DEL mutant had a stallforce at most 27% that of WT, results shown in Figure 24. The effects on the force-velocity behavior as a result of the mutations were also characterized by the authors and are presented in Figure 25. A Boltzmann model [16, 30] was used to fit the data and obtain further insights:

$$v(F) = \frac{v_{max}(1+A)}{1 + Aexp[\frac{F\delta}{k_B T}]}$$

v_{max} is the unloaded velocity given by $v_{max} = \Delta/(\tau 1 + \tau 2)$, $\Delta = 8.2nm$, $\tau 1, \tau 2$ are times associated with biochemical (load-independent) and mechanical (load-dependent) transitions at zero load. A is defined as $\tau 1/\tau 2$, δ is the effective distance over which the force acts, and $k_B T = 4\ pn * nm$. Results from this fit show that v_{max} was unaltered, whereas A and δ were increased for the kinesin mutants. Together with the applied loads, these results suggest that in the mutants, the kinetics of the load-dependent mechanical transition is affected by the disruption of the CNB. In the case of the mutants, it is likely that they rely heavily on thermal fluctuations and assisted loads in order to move. It has been suggested that the kinesin cycle is made up of >1 load dependent steps [16]. A fits to a Fisher-Kolomeisky [31] 2-state kinetic model (fits shown in Figure 24, B) shows that the reaction coordinates (one

for the power stroke leading and the other for a diffusive search) was equally divided in WT and skewed in 2G and DEL. These results suggest that in the mutants, there is a biasing of the reaction coordinate toward a state dominated by a diffusive search, further supporting the CS as a mechanism to control the powerstroke in kinesin.

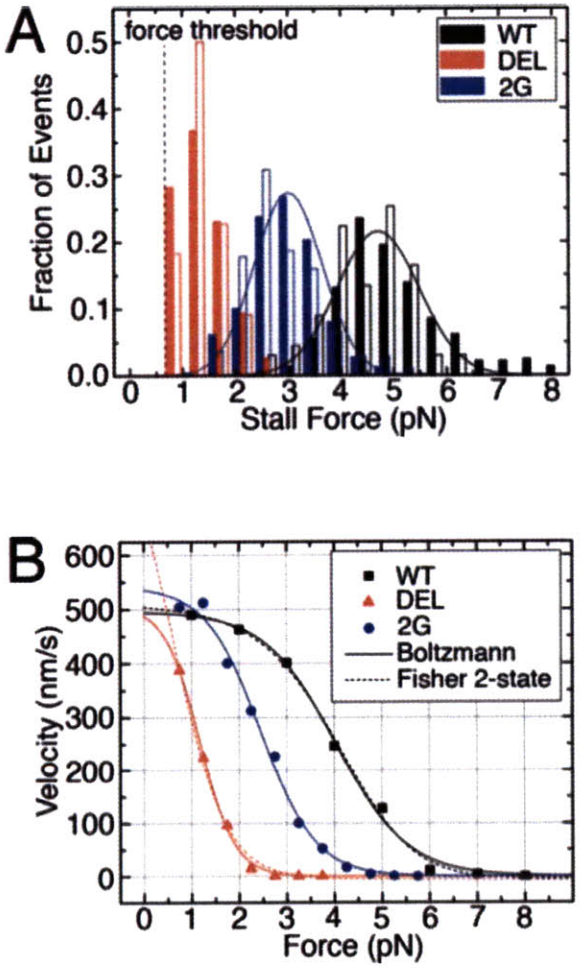

Figure 24: A) Stall force distributions for kinesins running under load. Solid lines measurements are at saturating 1mM ATP and open bars at limiting 4.2μM ATP. B) Force-velocity curves and fit to model. Dotted lines represent the Fisher 2-state model. Figures from [1].

Another important result outlined by the work of Khalil et al. was that of the effects of the mutations in the unloaded velocity of kinesin. Using a custom video tracking setup, it was determined that the 2G mutants had greater unloaded speeds v(0) and run lengths (l) when compared to WT kinesin. On the other hand, the DEL mutants had a slower unloaded velocity and shorter run lengths, results summarized in Table 3. The 2G increase could be explained, perhaps, with an additional state driven by a rapid formation of the CNB as a consequence of a more flexible CS. As for the DEL result, perhaps its motion is driven by thermal diffusion that gets rectified by microtubule binding.

		Load					No load	
		Blotzmann			Fisher 2-state			
Kinesin	Stall force,* F_s (pN)	v_{max},† nm/s	A†	δ,† nm	d_0, nm	d_1, nm	$v(0)$*, nm/s	L*, μm
WT	4.96 ± 0.05	493.7 ± 26.4	0.0043 ± 0.0050	5.53 ± 1.04	4.4	3.8	581.1 ± 38.8	1.104 ± 0.215
2G	3.02 ± 0.03	535.2 ± 27.8	0.0137 ± 0.0101	7.15 ± 1.10	1.1	7.1	608.2 ± 22.5	1.740 ± 0.209
DEL	1.37 ± 0.04‡	482.1 ± 33.5	0.0357 ± 0.0202	11.28 ± 1.24	0.4	7.8	254.8 ± 27.2	0.342 ± 0.088

Table 3: Summary of the results obtained by Khalil et al. [1]. Note WT has highest stall force.

2.6 Kinesin purification, more mutants and force clamp demonstration

As found by Khalil et al., mutations to the CS affect the folding transition required for kinesin to generate a powerstroke and push forward. It can be hypothesized that external assisting loads would recover the function of the DEL mutant and allow it to move in a manner similar to that of WT. Preliminary work was able to confirm that an applied force in DEL could indeed rescue its condition and make it more WT-like [4]. More results are needed to further characterize these mutants and further elucidate the mechanism by which they walk. To this effect, in the next sections we present a detailed overview of the

purification process to obtain kinesins from a plasmid inserted into e.coli. We also demonstrate a functional force clamp and show clamping traces of WT and 2G kinesin.

2.6.1 Kinesin Purification

In order to study kinesin (for all experiments we used a recombinant truncated derivative of kinesin made up of the N-terminal 401 aa of Drosophila melanogaster kinesin heavy chain (DmK401), a biotin carboxyl carrier proteim (BCCP) and a His6 tag) with the optical trap, protein aliquots were prepared as described in Appendix A.2. Briefly, BL21(DE3pLysS) *Escherichia coli* cells (Invitrogen) were transformed with 3 plasmids (WT, 2G and DEL) and grown in agar plates plus antibiotic for selectivity (+ Chloramphenicol, + Ampicillin). Cell cultures were grow in LB medium and later in TB medium at 37 C, supplemented with 24 mg/L biotin. Protein induction was carried out at a measured OD of 0.53-0.6 with the addition of 1 mM isopropyl-β-D-thiogalactopyranoside (IPTG) and the temperature lowered to room temperature (~ 23 C). 3 hours later, 0.2 mM of rifampicin was added and the culture allowed to grow for 12 hours. After, the cells were pelleted and the supernatant discarded. Cell pellets were immediately resuspended in Full Lysis Buffer (20 mM imidazole, pH 7, 4 mM MgCl2, 2 mM PMSF, 2 μg/ml pepstatin A, 20 μg/ml TPCK, 20 μg/ml TAME, 2 μg/ml leupeptin, 20 μg/ml soybean trypsin inhibitor, 10 mM β-mercaptoethanol). Lysates were then flash frozen in liquid nitrogen and expose to 3-4 freeze-thaw cycles. After this, lysates were incubates with 1 mg/ml RNase A (Sigma) and 0.5 mg/ml DNase 1 (Sigma) for 30 minutes in ice. Lysates were then centrifuged (21,800 x g) for 10 minutes and then ultracentrifuged (180,000 x g) for 30 minutes at 4 C. In order to isolate kinesin (HIS-tagged), liquid chromatography was carried out using a column with Ni-

NTA resin (Qiagen, Ni-NTA Superflow) and 70-100 mM imidazole elutions used to unbind the protein. Fractions were collected and ran on a SDS page gel to determine maximum protein yield (Figure 25). A Vivaspin 15 spin column (Vivascience, 30,000 MWCO) was used to concentrate protein and aliquots were stored at -80 °C in Kinesin Storage Buffer (50 mM imidazole, pH 7, 100 mM NaCl, 1 mM MgCl, 20 μM ATP, 0.1 mM EDTA, 5% sucrose).

Extensive characterization of the protein product was previously carried out in the work of Khalil et al. For the purpose of this thesis, we characterized kinesin by running a SDS page to confirm its purity and running several single-molecule bead assays to confirm motility.

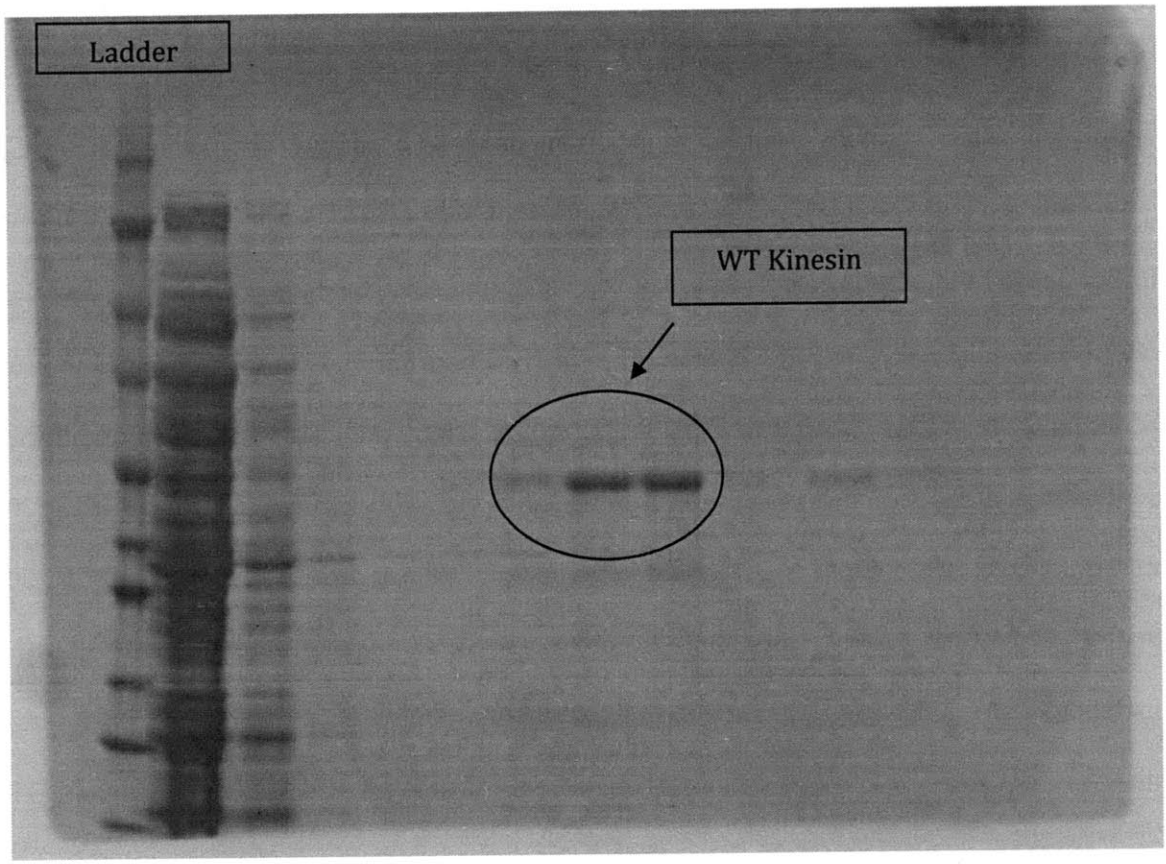

Figure 25: SDS Page showing kinesin.

2.6.2 Kinesin single-molecule bead assay and microtubule polymerization

A complete protocol for the single-molecule assay for kinesin is presented in the appendix A.3. Briefly, buffer solutions of PEM80 and PEM104 were prepared ahead of time. PemTax was prepared by combining PEM80 with 10mM Taxol in DMSO (Cytoskeleton inc.). Next, 1.5 mL of assay buffer was prepared (1300 µl PEM80, 3µl DTT, 3 µl Taxol, 15 µl 1M ATP, 25 µl K-acetate, 150 µl of 10 mg/ml Casein in PBS + Tween) and stored in ice. C-tax was also prepared (80 µl PemTax and 20 µl of 10 mg/ml Casein) and stored in ice. Streptavidin coated ~400 nm polystyrene bead (Spherotech) were prepared by first washing 4 times at 10,000 rpm for 6 min, reconstituting in PBS and then sonicating for 3 minutes at 40% power. Kinesin dilutions were prepared by mixing kinesin aliquots with Assay Buffer and storing in ice. Dilutions of up to 100,000X were made in order to reach the single molecule limit, when statistically there are fewer kinesin than beads in solution and 1 kinesin bound per bead. Kinesin dilutions were then incubated with the beads for an hour and an oxygen scavenging system added (glucose 100X oxidase, 100X catalase, 100 X glucose).

As part of this assay, microtubules were polymerizes as following the protocol in Appendix A.2. Simultaneously, glass cover slips were etched in KOH as described in Appendix A.4 and soaked with 300 ml Ethanol and 1 ml Polylysine (Sigma). Cover slips and double-sided tape were used to form a flow cell and the microtubules allowed to bind to the surface. High velocity flow of PemTax was used to align the microtubules along the flow channel and C-tax was used to block the surface so as to avoid non-specific interactions. The Kinesin-bead dilution was then flowed into a flow cell.

Once ready, the sample was placed under the microscope and the optical trap calibrated as previously described before. Trap stiffness was set to approximately 0.05pN/nm for all experiments. Figure 26 shows an illustration of the experimental setup.

Figure 26: Illustration of the kinesin bead assay. Beads tagged with kinesin are trapped with the optical trap [6]

2.6.3 Results

In order to test that kinesin was functional, a sample aliquot was tested after each purification batch of WT, DEL and 2G. Single-molecule bead assays were prepared as previously described and kinesin-coated beads trapped using an optical trap. All necessary calibrations were performed and the data was analyzed using custom software written in MATLAB (Appendix B). Kinesin dilutions were made and a kinesin per bead dilution was verified for WT and 2G kinesin as demonstrated by observing single 8nm steps (Figure 27,

Figure 28) at low ATP concentrations (4μM). DEL mutants were visually verified to be functional. Appropriate positioning of the bead over the microtubule was assessed after the acquisition of data by fitting a straight line to a X-Y plot of the bead position as determined by the PSD (Figure 29). All data was filtered using a Savitzky-Golay filter.

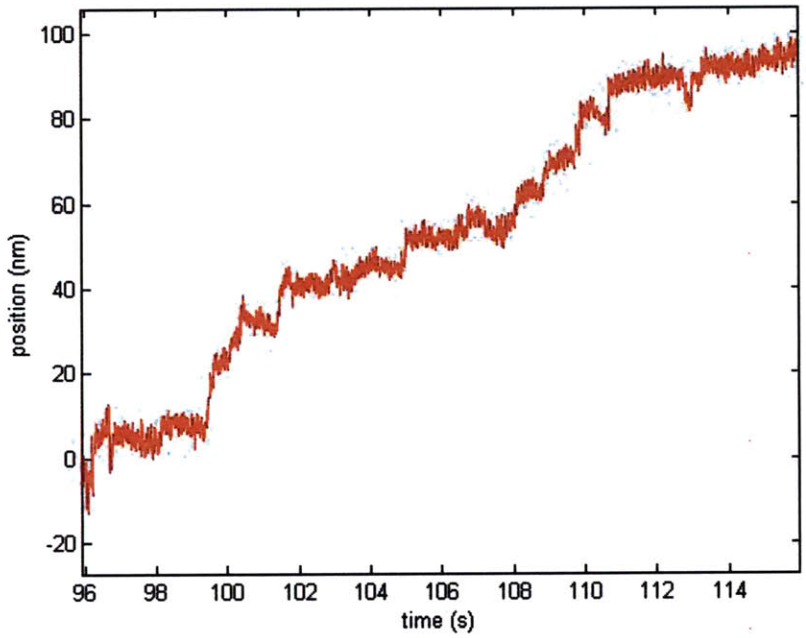

Figure 27: Bead position as a function of time. Beads were tagged with WT kinesin. Note the kinesin characteristic 8 nm steps.

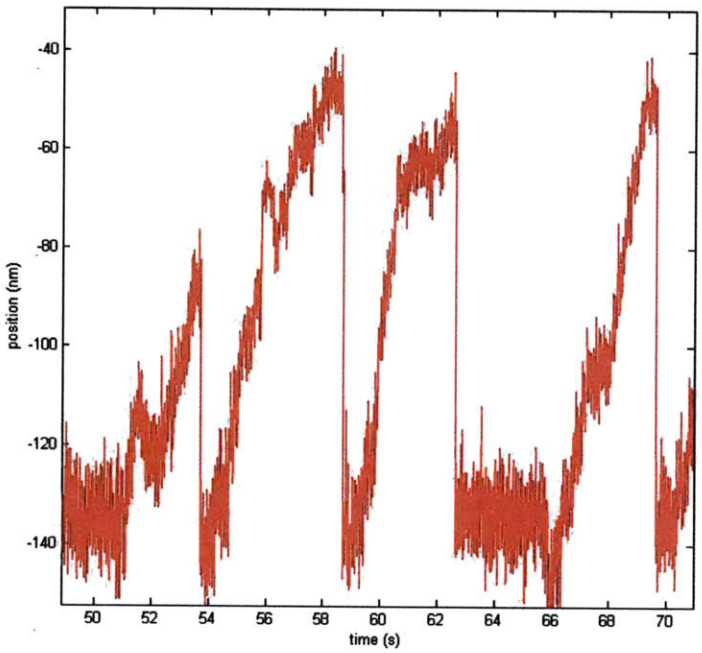

Figure 28: Bead position as a function of time. Beads were tagged with 2G kinesin. Note length of the run and the characteristic "snap back".

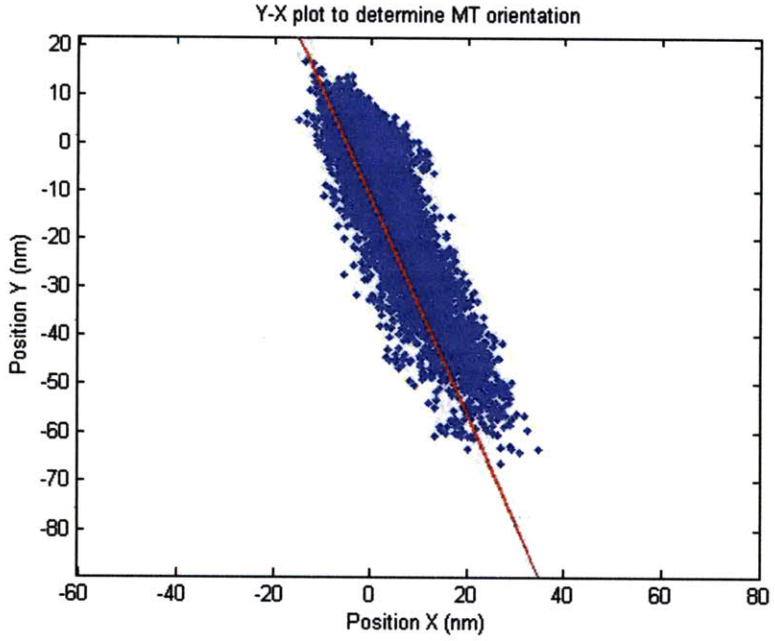

Figure 29: The blue dots represent the average bead position and the red line is a least square fit of the position and indicates the microtubule orientation.

As part of this phase in the project, we also tested the force clamp to ensure that it worked properly and was able to follow kinesin under both forward and backward loads. Figure 30 shows a 10 second trace of the force clamp in action clamping WT kinesin. Figure 31 shows a trace of forward load and Figure 32 a trace of backward loads. Both traces were done with a stiffness of 0.06pN/nm.

As for future work, the force clamp can be configured to apply sideway loads and can be modified to accommodate future 2D force clamping experiments. In addition, with the force clamp presented in this work can be used to study motility in future kinesin motors with different mutations to the CNB.

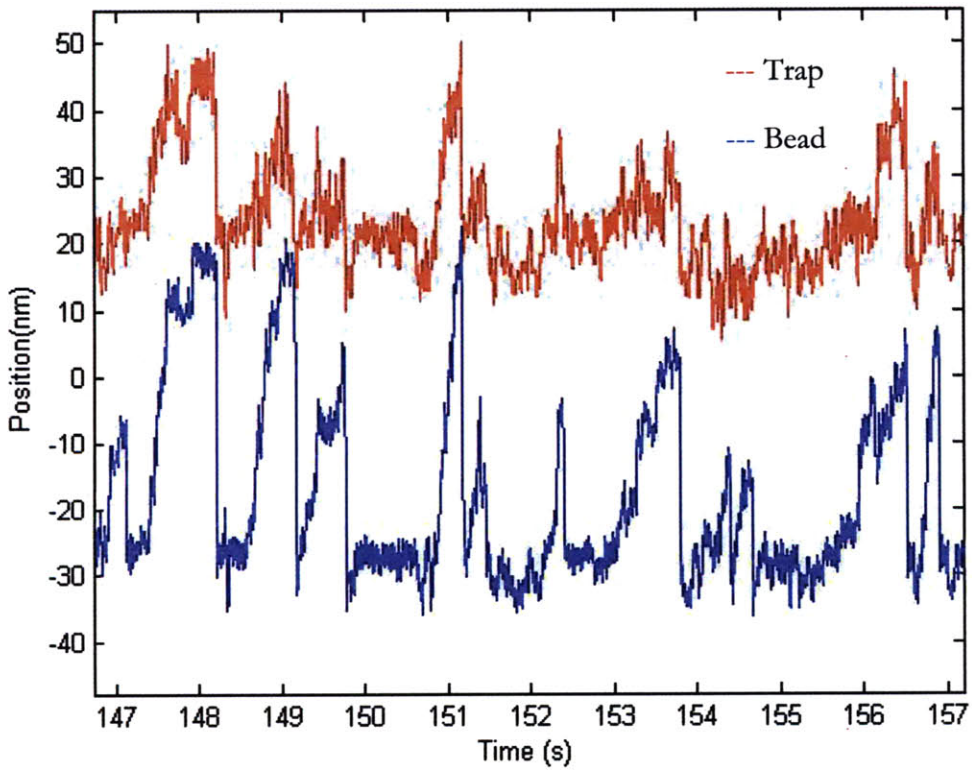

Figure 30: Beads tagged with WT kinesin moves under a force clamp. In this case, the optical trap in red leads the bead, indicating an applied forward load.

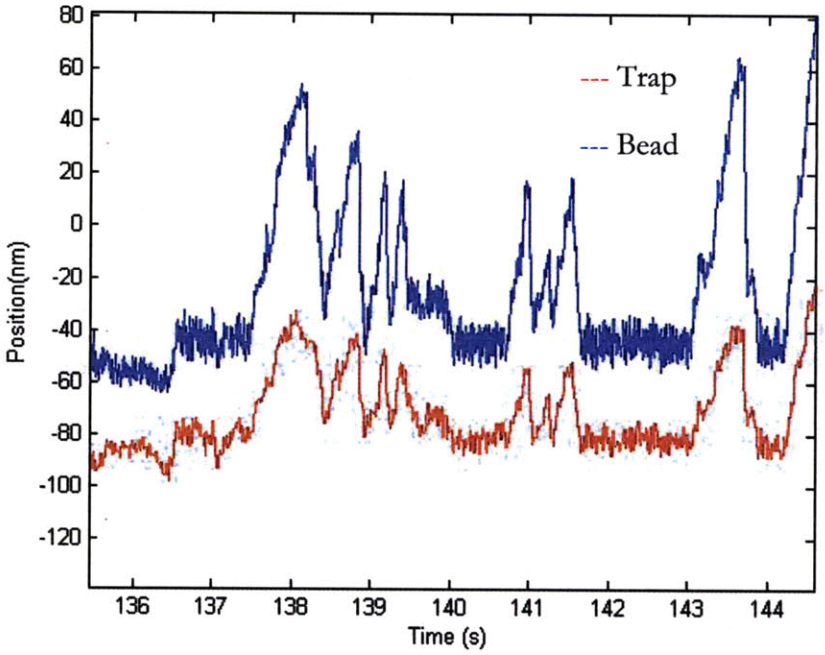

Figure 31: Beads tagged with WT kinesin moves under a force clamp. In this case, the bead in blue leads the optical trap in read, indicating an applied backward load.

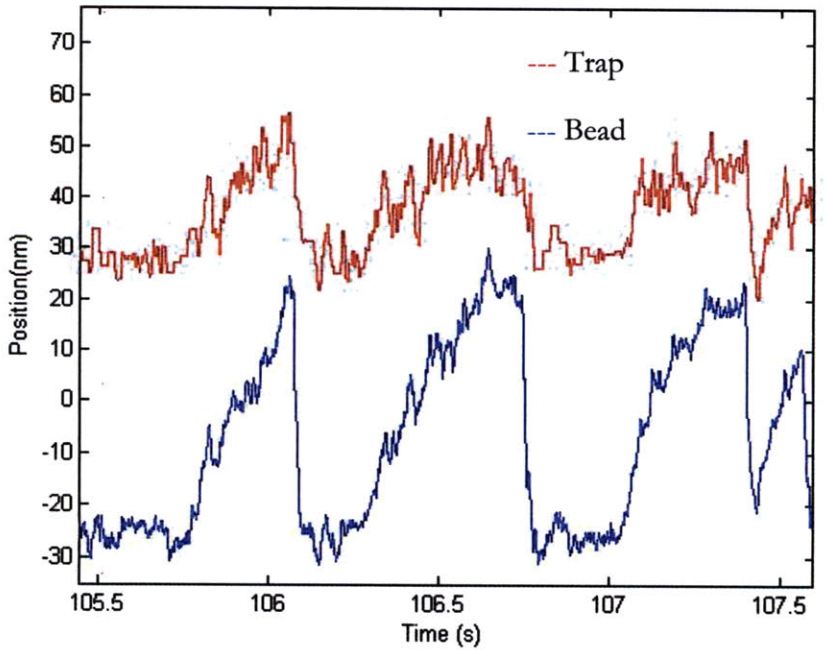

Figure 32: A close look at clamping. Notice how the trap, in red, does not step as smoothly as kinesin yet is able to follow.

Chapter 3

Tools for the study of the kinesin – e-hook interaction and initial findings.

3.1 Introduction

Understanding how the kinesin motor head and the binding site in the microtubule interact is an important step to fully realize a model of kinesin walking. Kinesin is a highly-processive motor, that is, can stay attached to microtubules over long distances without dissociating. Previous work has demonstrated that kinesin hydrolyses one ATP molecule per 8 nm step while the motor heads alternate between an ADP state and an ATP bound state [33]. A complete picture of how this process occurs is lacking, that is, how does kinesin alternate between ADP and ATP state? How is the ADP affinity controlled when finding the next microtubule binding site? Preliminary simulations by Hwang and Lang (unpublished) suggest that the dynamic aspect of how the trailing head detaches from the microtubule and lands on the binding site are mediated by the flexible C-terminal E-hook of the microtubule.

In this section we present new tools to study the kinesin – e-hook interaction and propose further experiments.

3.2 The E-hook

Microtubules are made up of α-β tubulin heterodimers. Dimers form protofilaments, and these in turn group in sets of 13 to form a microtubule [34]. Within the microtubule is the E-hook. The E-hook is formed by the last 10-18 C-terminal residues of α-β tubulin. The E-hook is negatively charge as it is rich in aspartic acid and glutamic acid [35]. Previous work has shown that proteolytic cleave of the E-hook can affect kinesin processivity [35-37] by affecting the ADP dependent binding to the microtubule. Furthermore, E-hook cleavage does not seem to affect the strong binding state of the motor head or the stall force.

There is evidence to suggest that the E-hook interacts with kinesin's neck coiled-coil [37]. In their experiments, Thorn et al. mutated the kinesin neck coiled-coil in order to make it more positively or negatively charged. In the case of added positive charge, kinesin was showed increases processivity, with negative charge having the opposite result. Furthemore, in the presence of high-salt concentration or removal of the E-hook diminishes kinesin processivity. Previous work also fit in quite well with this finding, as deletion of the neck coiled-coil also reduces procesivity [38]. Recent work by Lakamper et al. [39], however, has shown that in experiments with *Neurospora crassa* kinesin, which lacks positive charges in the neck and thus should not interact with the E-hook of α tubulin, motility is affected by the proteolytic removal of the E-hook [35]. Furthermore, cryo-EM analysis of the bound head suggests that the E-hook of β tubulin may be involved in the process of capturing the moving motor head [40]. When combined, these results seem to favor an interaction between the kinesin motor head and the E-hook during motility.

3.3 E-hook peptides and assays

To directly probe the nature of the kinesin motor head and e-hook interaction, we developed 2 assays: one based on binding E-hooks to the surface of a flow cell and another based on the kinesin based assays. We used the optical trap to study kinesin motility with hopes to uncover any weak interactions that may arise as a result of bead – e-hook binding or change in kinesin stall force.

3.3.1 E-hook peptides

In order to obtain isolated E-hook peptides to perform single molecule experiments, we utilized the services of the M.I.T. Biopolymers facility to synthesize 3 E-hook peptides shown in Table 4:

ID		MW	N-Term	Sequence	C-term
E-Hook#1	+ Biotin	2083.72	NH2 - Biotin	A-T-A-D-E-Q-G-E-F-E-E-E-G-E-E-D-E-A	COOH
E-Hook#2	Wild-Type	1983.72	NH2	A-T-A-D-E-Q-G-E-F-E-E-E-G-E-E-D-E-A	COOH
E-Hook#3	+ C-G-G	1957.65	NH2	C-G-G-D-E-Q-G-E-F-E-E-E-G-E-E-D-E-A	COOH

Table 4: E-hook peptides.

E-hook #1 was modified with the addition of a Biotin in order to perform Biotin-Streptavidin binding assays and facility binding to a surface. E-Hook #2 is wild-type peptide

and E-Hook #3 contains an N-terminal cysteine that could be linked to DNA using a sulfo-SMCC linker in future tethering experiments.

3.3.2 Peptide-Surface Assay

In order to study the Kinesin – E-Hook interaction, we first designed an assay in which we attached an E-Hook to the surface of a glass flow cell and then flowed in beads tagged with kinesin. Figure 33 shows a schematic of the experimental setup. We decided to use Polyethylene glycol (PEG) coated glass cover slips for a variety of reasons. First, PEG is commercially available bound to a Biotin molecule, and second, when placed on a surface it has been successfully used to eliminate non-specific binding [41]. PEG is also convenient as it has no charged groups, thus not likely to interact with the negatively charged E-hook.

For this experimental setup, glass cover slips (Corning) were PEGylated as described in Appendix A.6 using PEG tagged with a Biotin (Laysan Bio, Inc) and having a MW of 5,000. Streptavidin at a concentration of 1 mg/ml was flowed in and allowed to bind for at least 10 minutes. Next, E-hook #1 (Biotin tagged) at a concentration of approximately < 2.5 mM in Pem80 was flowed in and incubated for at least 15 minutes. The exact concentration for E-hook was difficult to determine, thus we provide an upper bound value and address this issue later. In order to reduce the likelihood of any non-specific interactions between the surface and the kinesin beads, 20 μL of 100 mg/ml Casein (Sigma) on PBS was flowed, incubated for 10 minutes, and excess Casein washed with 80 μL of Kinesin Assay Buffer. We next added 20 μL of ~ 400 nm beads tagged with kinesin into the flow cell. The final sample was placed under the microscope in order to observe the formation of tethers. The optical trap was used to distinguish non-specifically bound beads from possible tethers as the latter are firmly bound and require forces in excess of 5 pN to remove. The number of beads per

field of view was noted. As a control, a second sample that did not include the E-Hook was prepared in parallel.

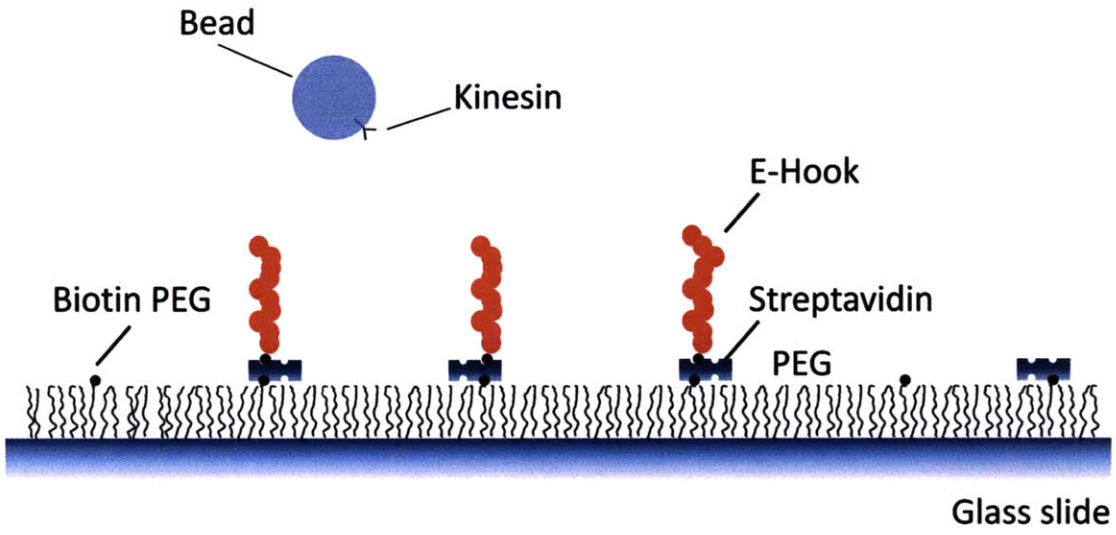

Figure 33: Peptide-surface assay. E-hook peptides were bound to a glass surface via a Biotin-Streptavidin bond. The glass surface was previously coated with PEG.

3.3.3 Kinesin Bead Assay with E-hook

Kinesin tagged to beads through a Biotin-Streptavidin bond were prepared as previously described. PemTax, Assay Buffer and C-tax were freshly prepared and kept in ice. Glass cover slips were etched in KOH (Appendix A.5), coated with Polylysine (Sigma) and dried in a 90 °C oven for 15 minutes. 2G mutant kinesin stocks were diluted up to 100,000X in Assay Buffer and incubated for one hour with beads. E-hook was added to for an approximate final concentration < 6 mM. As a control, an additional flow cell that did not include E-hook#2 was prepared. A schematic of the assay is shown in Figure 34.

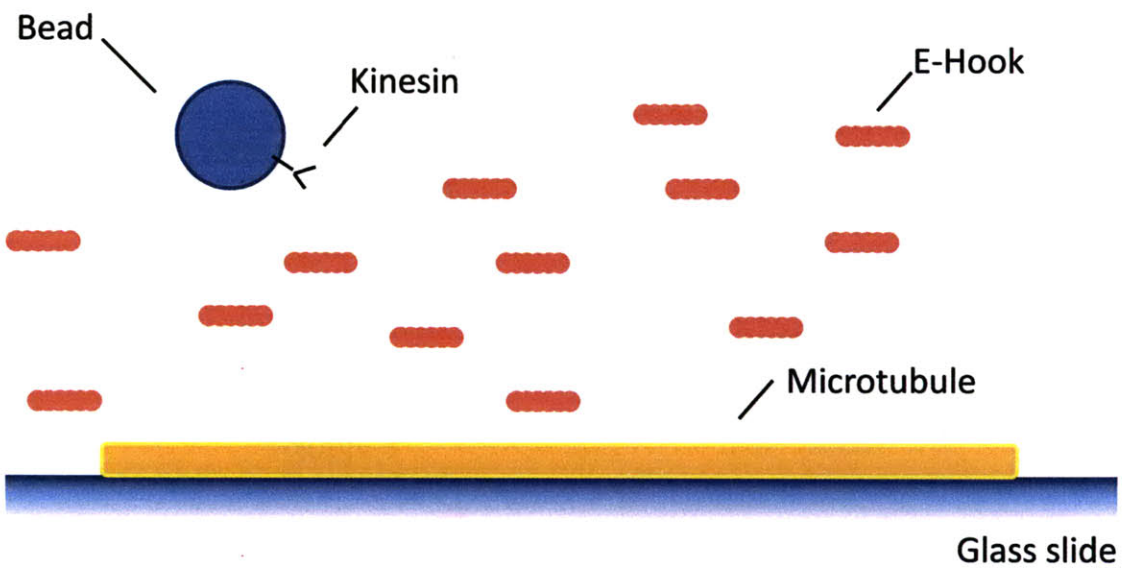

Figure 34: Kinesin bead assay with. E-hook peptides were flowed into solution after kinesin was tagged to Streptavidin coated beads.

After sample preparation, the optical trap was calibrated in order to set the stiffness at about 5 pN/nm. Beads were trapped and placed over the microtubules. Kinesin runs were first detected visually and then confirmed with custom made software written in Labview. Voltage traces from the PSD were recorded at 20 kHz and filtered using an analog low pass filter with a 2 kHz corner in order to eliminate high frequency noise. The acquired data was then analyzed with custom written MATLAB software (Appendix B).

After the data was collected and converted from voltage into position, it was plotted and manually inspected. In short, exerted forces over 1pN were considered kinesin runs and the point where the force was maximum and with a sharp transition was defined as the stall force. All stall forces were then plotted in a histogram. Other statistics such as the variance and velocity for a run can be determined from this data if needed. Figure 35 shows a sample trace of the analyzed data.

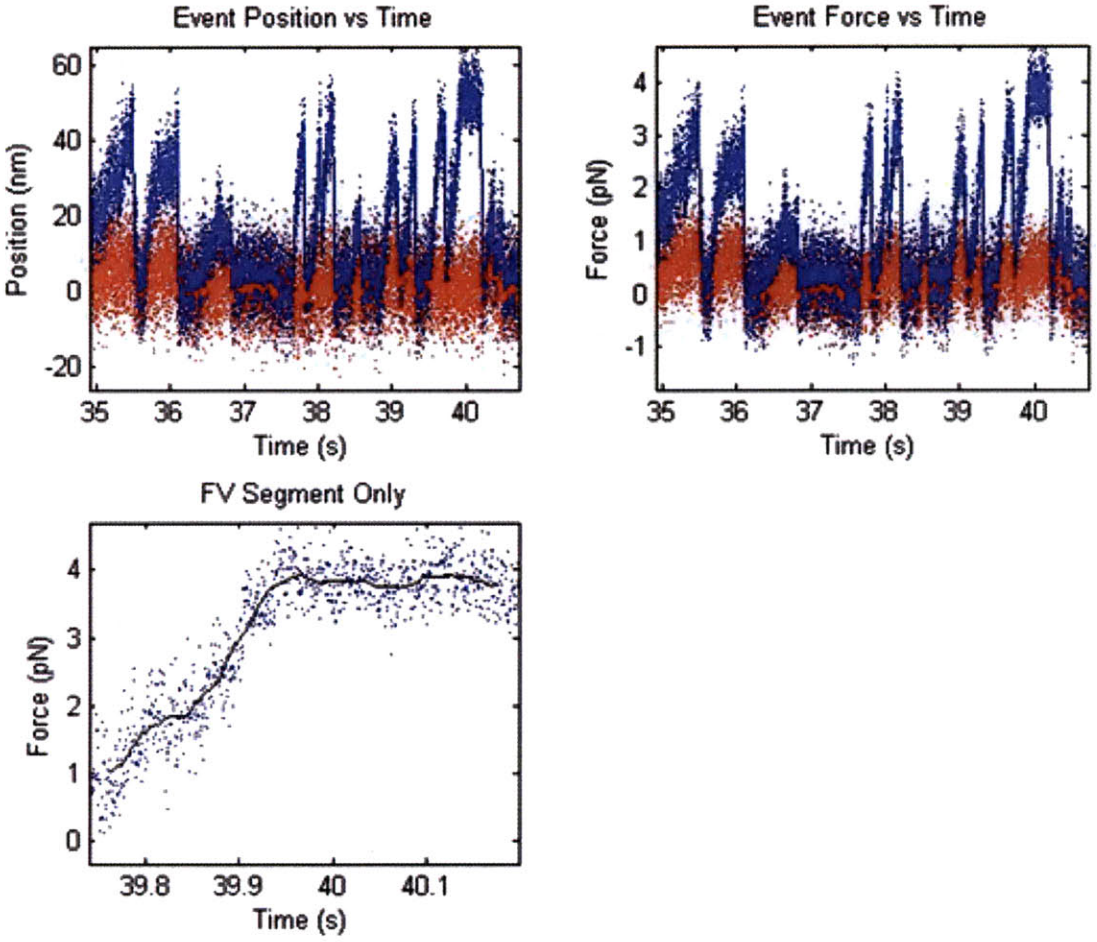

Figure 35: Sample run of the kinesin data analysis. Notice how on the Force vs Time plot how 2G kinesin stalls at about 4 pN.

3.3.4 Results and Discussion

We first performed the peptide-surface assay with WT kinesin. At a first glance, both experiments, with E-hook bound to the surface and control, looked similar as determined by the number of beads stuck to the surface. 10 fields of view were examined under bright field for each sample and the results presented in Table 6. Note that a field of view represents an estimated area of ~100 μm*μm. Using the optical trap at a stiffness of approximately 0.05 pN/nm, we pulled on surface bound beads. Despite the applied forces of up to 5 pN, as determined by the distance from the trap center to the bead, we were unable to detach beads. These results suggest that stuck beads were most likely non-specifically bound to the surface and not a result of kinesin – e-hook interactions.

Column1 Field of View #	E-hook No. Beads	Control No. Beads
1	3	1
2	0	0
3	4	0
4	0	1
5	0	2
6	0	0
7	2	0
8	1	3
9	0	1
10	0	0
Mean	1	0.8
Std Dev	1.49	1.03

Table 5: Number of beads stuck to the surface both with E-hook and in control experiments.

The kinesin bead assay with E-hook was prepared using the kinesin 2G mutant. The goal of this experiment was to observe and quantify any interaction between kinesin and the

E-Hook in solution. The idea was to test whether, during stepping and subsequent diffusive search after the powerstroke, the kinesin motor head would interaction with an E-hook in solution causing kinesin to fall of the microtubule and this would be reflected as having a lower stall velocity and speed. We were also interested in observing kinesin steps and any behavior out of the ordinary such as back-steps. The rationale behind using 2G, as opposed to WT, was that because of its lower stall force and enhanced unloaded velocities, we hypothesized that it would be more susceptible to any interactions with the E-hook in solution. We used the optical trap to capture beads and later analyzed the data in order to determine stall forces. For the E-hook concentrations we provided an approximate upper limit as exact e-hook product obtained from the M.I.T. Biopolymer facility were not purified (Synthesis Scale 5 μmol) and product quantities small. For future experiments, HPLC purification and aminoacid analysis should be carried out in order to determine more precise concentrations. In addition, creating e-hook samples with a tagged dye such as a TAMRA could help visualize single peptides bound to the surface or in solution in future experiments using the assays described in this thesis.

Figure 36 and Figure 37 show stall-force distributions for 2G kinesin running with and without E-hook (control) present in solution. The mean stall force was found to be 3.18pN in the presence of E-hook in solution and 3.25 pN in the control experiments. The data was fit to a single exponential Gaussian and the distribution details shown in Table 6:

Experiment	No. Samples	Mean Stall Force Fit	Std Dev
+ E-hook	107	3.161	1.098
- E-hook	90	3.02	1.109

Table 6 Stall force results.

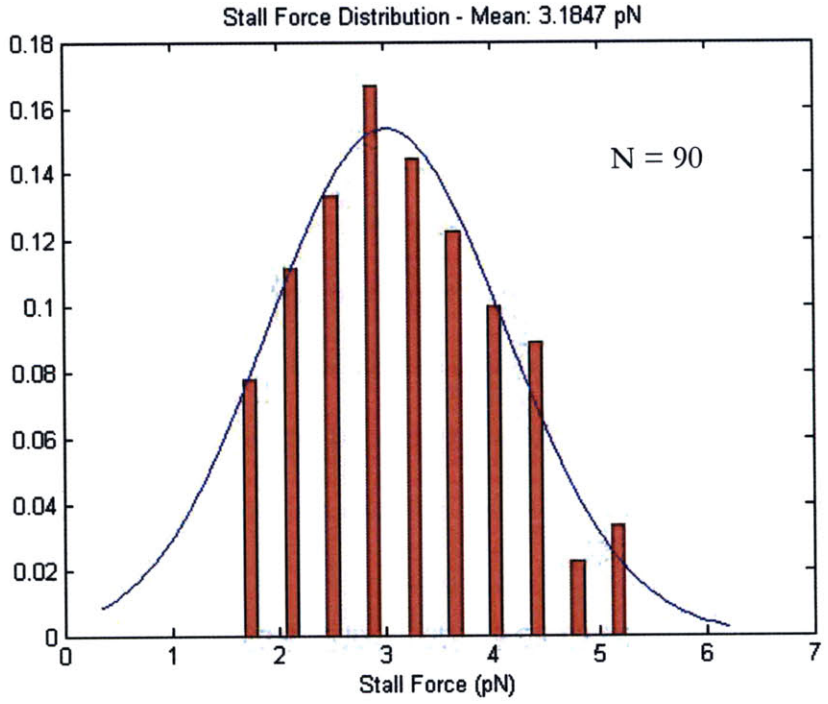

Figure 36: Stall-force distribution for 2G kinesin without E-hook in solution (control).

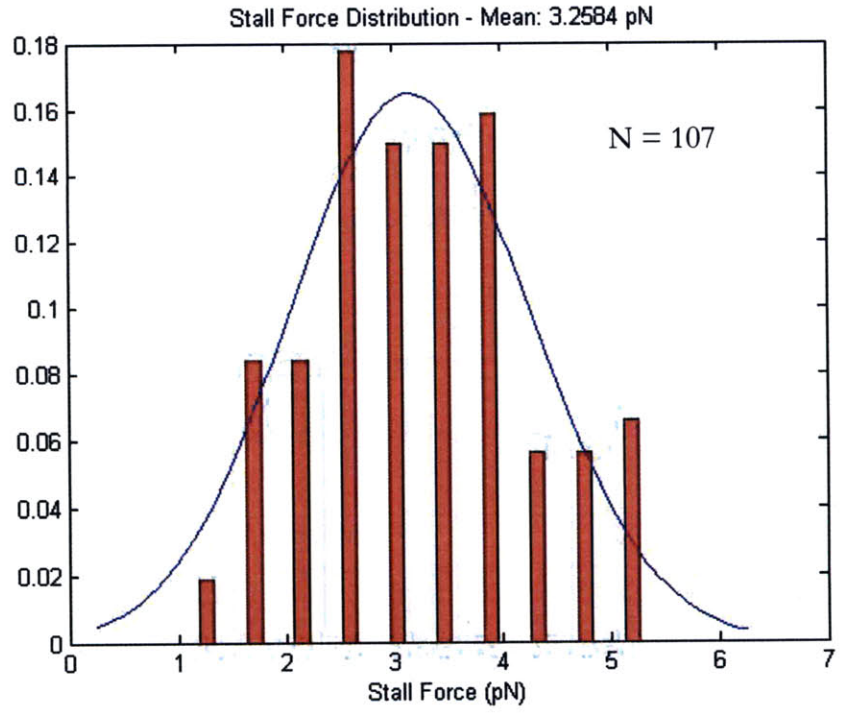

Figure 37: Stall-force distribution for 2G kinesin with E-hook in solution.

Our results indicate that in the presence of E-hook at the estimated concentration range, 2G kinesin is functional and its stall force is approximately 3 pN. Our stall force measurements match those previously reported by Khalil et al. [1], indicating that the mean kinesin stall force is unaffected by the presence of e-hook in solution. Further experiments are required, however, to conclusively uncover the role of the E-hook in assisting kinesin motility. For instance, one such experiment that could be performed would be to setup kinesin motility experiments while flowing e-hook in solution at ever increasing concentration on a coverslip or PDMS chip. From this experiment, one could quickly scan several conditions in search for a kinesin- e-hook interaction. Another experiment could be to study kinesin running over microtubules with cleaved e-hooks. While the preliminary results presented in this work do not conclusively uncover the nature of an interaction between kinesin and the e-hook at the single molecule level, they do give rise to many new questions. For instance, is it possible that the interaction between kinesin and the e-hook occurs at a fast rate? How come the stall force remains unchanged? Is kinesin not interacting with the e-hooks in solution? It may be possible that the concentration we used for e-hook in solution is much lower than the local concentration of e-hook, thus unable to compete for the motor. It could also be that the powerstroke forces kinesin to the binding site regardless of the presence of e-hook. As future experiments, it will be interesting to further increase the concentration of E-hook (which seems to be readily soluble in buffer) and repeat these measurements using the methods described in this thesis. Answer to the many new questions that arise from the work presented here, and many more that will come up as we learn more about kinesin, make it an exciting time to study kinesin at the single molecule level.

Appendix A

Kinesin Protocols

A.1 Tubulin Polymerizing Protocol

Adapted from Ahmad Khalil.

Materials

1) PEM80. 6.048 g Pipes (Sigma P-1851), 95.1 mg EGTA (Sigma E-4378), 204.1 μL of 4.9 M MgCl2 (Mallinckrodt H590) stock into 250 mL final volume (80 mM Pipes, 1 mM EGTA, 4 mM MgCl2, pH adjusted to 6.9 with KOH).

2) PEM104. 3.133 g Pipes (Sigma P1851), 49.452 mg EGTA (Sigma E4378), 128.57 μL of 4.9 M MgCl2 (Mallinckrodt H590) stock into 100 mL final volume (103.6 mM Pipes, 1.3 mM EGTA, 6.3 mM MgCl2, pH adjusted to 6.9 with KOH).

3) STAB. 34.1 μL PEM80, 5 μL 10 mM GTP (Cytoskeleton BST06), 4.7 μL 60 g/L NaN3 (Sigma S-8032), 1.2 μL 10 mM Taxol (Cytoskeleton TXD01), 5.0 μL DMSO (Sigma D-5879).

4. Tubulin (Cytoskeleton T237).

Protocol

1) Spin tubulin for 30 min. at 4 C.

2) Combine 15.2 μL PEM104 + 2.0 μL 10 mM GTP to make PEM/GTP solution.

3) Combine 15.2 μL PEM/GTP + 2.2 μL DMSO, vortex mixture, then add 4.8 μL of 10 mg/mL tubulin to make TUB solution.

4) Place TUB solution in water bath at 37μ for 30 min.

5) Remove TUB from water bath and add 2 μL of STAB.

6) Store microtubules at room temperature.

A2. Kinesin Expression and Purification

Adapted from Ahmad Khalil.

Materials

1) LB Broth (with 100 μg/mL ampicillin (amp) + 25 μg/mL chloramphenicol (chlr)).

2) LB Plates (with 100 μg/mL amp + 25 μg/mL chlr).

3) TB Broth. Add 47.6 g TB (Difco Terriμc Broth) and 4 mL glycerol into 1 L ddH2O and autoclave. Once cooled, add antibiotics (μnal: 100 μg/mL amp + 25 μg/mL chlr) + biotin (100 μM, 24 mg).

4) 1 M IPTG. In water stored in 1 mL stocks at -20μ.

5) Rifampicin (20 mM, 16.5 mg/mL in methanol, 100X stock, stored at -20μ in 1 mL aliquots).

6) Lysis Buffer (20 mM imidazole, pH 7, 4 mM MgCl2). Add 0.680 g imidazole and 0.5 mL of 4 M MgCl2 into 500 mL ddH2O.

7) β-mercaptoethanol (Neat liquid, room temperature).

8) PMSF (Sigma P7626). 200 mM in dry isopropanol, store at -20μ.

9) Pepstatin A (Sigma P4265). 5 mg/mL in DMSO, store at -20μ.

10) TPCK (Sigma T4376). 10 mg/mL in DMSO, store at -20μ.

11) TAME (Sigma T4626). 40 mg/mL in ddH2O, store at -20μ.

12) Leupeptin (Sigma L9875). 5 mg/mL in ddH2O, store at -20μ.

13) Soybean TI (Type I-S, Sigma T9003). 10 mg/mL in ddH2O, store at -20μ.

14) DNAse I (solid, Grade II, Sigma D4527).

15) RNAse A (solid, Type II-A, Sigma R5000).

16) Ni-NTA Resin (Qiagen Ni-NTA Superow).

17) TCEP (Molecular Probes T-2566). 10 mM in ddH2O prepared immediately before

use.

18) Vivspin 15 Spin Column (Vivascience VS1522, 30,000 MWCO).

19) Protease Inhibitor Cocktail, PI. Prepare 4 mL of PI and store at -20μ in 250 μL aliquots:

Stock	Final Concentration (mg/mL)	Volume (μL)
Pepstatin A	0.2	160
TPCK	2	800
TAME	2	200
Leupeptin	0.2	160
Soybean IT	2	2
ddH2O		1880

20) Econo-Column Chromatography Columns (Bio-Rad, Cat No. 737-1512, 1.5 x 10 cm, 18 mL).

21) Bradford Reagent (Sigma B6916).

22) NuPAGE 4-12% Bis-Tris Gels (Invitrogen, Cat No. NP0321BOX, 1.0 mm x 10 well).

23) Kinesin Storage Buffer (50 mM imidazole, pH 7, 100 mM NaCl2, 1 mM MgCl2, 20 μM ATP, 0.1 mM EDTA, 5% sucrose).

Day 0

1) Streak out fresh colonies of kinesin expressing E. coli (WT K401-BIO-H6 is called KT2) on LB plate (+amp, +chlr). Grow overnight (12{16 hrs) at 37μ and store parafilmed plate at 4 C for up to one week.

Day 1

1) Pick single colony and inoculate 20 mL of LB broth (+amp, +chlr) in sterilized 250 mL flask.

2) Grow overnight (12-16 hrs) in 37 C shaker.

Day 2

1) Inoculate 500 mL TB broth (+amp, +chlr, +biotin) with 5{10 mL volume of the LB overnight culture (time = 0). Grow culture in 37μ shaker and record OD600 measurements.

2) Induce expression at OD600 = 0.53{0.60 by adding 1/1000 volume of 1 M IPTG stock (final concentration 1 mM). Upon induction, reset thermostat to 22μ.

3) Add 1/100 volume of 20 mM rifampicin stock (5 mL into 500 mL culture) 2 hrs. after induction.

4) Keep culture shaking at 22 C in a shaker overnight (12-20 hrs.).

Day 3

1) Pellet cells by centrifugation (5,000g, 4μ, 10 min.).

2) To Lysis Buffer, add β-mercaptoethanol (final concentration 10 mM), 1/100 volume of PI, and 1/100 volume PMSF. This makes Full Lysis Buffer. Make 5 mL for each 500 mL culture.

3) After the spin, drain supernatant as much as possible and retain cell pellets. Resuspend pellets in 5 mL Full Lysis Buffer1. Dispense resuspension into sterilized 15 mL Falcon tube for freezing.

4) Incubate cell suspension 30 min. on ice, mixing occasionally (internal lysozyme degrades cell wall). A general rule is 100-150 μL buffer per 100 mg pellet

5) Freeze suspension in 5 mL aliquots in liquid nitrogen. The frozen mixture is stored at -80 °C at least overnight.

Day 4

1) Thaw frozen cells (5 mL) with alternating brief (2 min.) exposure to 37 C water bath with agitation followed by brief (2 min.) cooling on ice. The solution should never rise signifcantly above ice temperature. At the point of complete thawing, refreeze the cells in liquid nitrogen. This process is repeated for a total of three thaws. Mixture becomes viscous and slightly darker in color.

2) Add 500 μL 10 mg/mL RNAse (μnal concentration 1 mg/mL) and 250 μL 10 mg/mL DNAse (final concentration 0.5 mg/mL). Incubate on ice for 30 min., with occasional mixing. The viscosity should decrease.

3) Spin at 21,800g for 20 min. at 4μ to retain low-speed-supernatant (LSS).

4) Equilibrate 2 mL of Ni-NTA resin in Full Lysis Buffer.

5) Spin LSS at 180,000g for 30 min. in Beckman ultracentrifuge at 4μ to retain highspeed-supernatant (HSS).

6) Mix HSS with Ni resin and incubate at 4μ for 1{1.5 hrs. (or overnight) on a rotator.

Day 5

1) Prepare chromatography column by washing with ddH2O and then Full Lysis Buffer.

2) Prepare 250 mL of Elution Buffer 1 (20 mM imidazole, 4 mM MgCl2, 10 mM β-mercaptoethanol (175 μL)) and Elution Buffer 2 (500 mM imidazole, 4 mM MgCl2, 10 mM β-mercaptoethanol (175 μL).

3) Mix Elution Buffers to obtain Final Elution Buffers:

Final [imidazole] (mM)	Elution Buffer 1 (mL)	Elution Buffer 2 (mL)
70	8.96	1.04
100	8.33	1.67
150	7.29	2.71
200	6.25	3.75
500	0	10

4) Load the mixture onto the column and collect the flow-through (Ni-FT) by gravity in the cold room.

5) Wash the column with Full Lysis Buffer until you get a at baseline, as measured by the Bradford Reagent2.

6) Elute and collect fractions with 10 mL volumes of increasing concentration of Final Elution Buffer. Note, for each elution, the μrst 2 mL of collected fraction actually correspond with the previous imidazole concentration (i.e., after applying 10 mL of 150 mM imidazole, the μrst 2 mL of collected fraction belong with the 100 mM imidazole fraction).

7) Run the fractions in separate wells of a SDS-PAGE gel and pool the fractions with significant, pure kinesin content.

8) Concentrate the pooled protein samples by spinning in a Vivaspin concentrator.

9) While concentrating, exchange Buffer so that the μnal protein solution is in Kinesin Storage Buffer.

10) Aliquot final protein solution into 5-10 μL volumes, freeze in liquid nitrogen, and store at -80 °C. Load a 96-well plate with small volumes of Bradford Reagent. Then apply 5-10 μL of Ni-FT to a well and approximate protein content by Bradford Reagent color change.

A.3 Kinesin Bead Assay

Adapted from Ahmad Khalil.

1) Make PemTax

(a) Label a tube PemTax, and add:

i. 1000 μL Pem80 (stored in 4 C)

ii. 2 μL Taxol (10 mM in DMSO, aliquots in -20μ)

(b) Store at RT

2) Make Assay Buffer

(a) Label a tube AB, and add:

i. 1304 μL Pem80

ii. 3 μL DTT (0.5 M in 10 mM K-acetate, aliquots in -20μ)

iii. 3 μL Taxol

iv. 15 μL ATP (100 mM in PEM80, aliquots in -80 °C)

v. 25 μL K-acetate (3 M, stored in 4 C)

vi. 150 μL 10 mg/mL Casein in PBT (made fresh once per week and stored at 4μ)

(b) AB final concentrations: 0.1 mM DTT, 20 μM Taxol, 1 mg/mL Casein, 1 mM ATP3, 50 mM K-acetate

(c) Store on ice

3) Make C-Tax

(a) Label a tube C-Tax, and add:

i. 80 μL PemTax

ii. 20 μL 10 mg/mL Casein

(b) Store on ice

4) Make bead dilution

(a) Dilute 20 μL 0.44 μm Streptavidin-coated beads (Spherotech, Cat No. SVP-05-10, 1.0% w/v) into 80 μL PBS

(b) Wash 4 times at 10,000 rpm for 6 min, reconstituting in 100 μL PBS

(c) Sonicate for 2 min at 40%

(d) Label a tube EM/AB, and add:

i. 4 μL beads

ii. 196 μL AB

5) Make Kinesin dilutions

(a) K/100: 2 μL K into 98 μL AB

(b) K/1000: 10 μL K/100 into 90 μL AB

(c) . . .

6) Make Kinesin/Bead dilution (KDB)

(a) Label a tube KDB/###, and add:

i. 50 μL EM/AB

ii. 50 μL K/###

(b) Incubate for 1 hour on the rotator at 4μC

7) Prepare Polylysine - coated coverslips, if not already done

(a) Dilute 1 mL Poly-L-Lysine into 300 mL EtOH and mix in 1 L beaker

(b) Place a rack of KOH etched coverslips into the solution, and let sit for 15 min

(c) Dry for 15 min in the oven

8) Make MT/50 - MT/150 dilutions in PemTax and start warming C-Tax and AB to RT

9) Add Glucose Oxidase plus Catalase to each KDB incubation

(a) Add 1 μL 100X Glucose oxidase4 (25 mg/mL in PBT, 10 μL aliquots in -80 °C)

(b) Add 1 μL 100X μ-D-glucose (500 mg/mL in PBT, 10 μL aliquots in -80 °C)

(c) Add 1 μL 100X Catalase (3 mg/mL in PBT, 10 μL aliquots in -80 °C)

10. Prepare flow channels from Polylysine-coated coverslips

(a) Flow in 15 μL MT/###, and let bind for 10 min

(b) Wash in 20 μL PemTax with high velocity

(c) Wash in 15 μL C-Tax, and let coat for 5 min

(d) Wash in 50 μL PemTax

(e) Wash in 80 μL AB

(f) Wash in 20 μL KDB/###

A.4 Etching glass coverslips

Adapted from Polly Fordyce and David Appleyard.

Etching coverslips removes the wax layer on the glass, enhances adhesion, and reduces back ground fluorescence.

Materials

1) 100 g KOH

2) Ethanol

3) MilliQ DI H2O

4) Corning Coverglass (22 x 40 mm) No. 1.5

Procedure

1) Dissolve 100g of KOH in 300 mL of Ethanol (takes about 30 minutes) in a 1 L beaker

2) Load teflon coverslip racks with coverglass

3) Fill 2 more 1 L beakers with 300 mL DI H2O and degas for 5 minutes

4) Fill one more 1 L beaker with 300 mL ethanol

(a) Degas this beaker and the ethanol/KOH beaker for 5 minutes

5) Submerge one coverslip rack in the KOH/ethanol solution and sonicate for 5 minutes

6) Wash coverslips by dipping the rack up and down and spinning it in the ethanol beaker

7) Wash coverslips by dipping the rack up and down and spinning it in the DI H2O beaker

8) Submerge coverslip rack in the second DI H2O beaker and sonicate for 5 minutes

9) Spritz coverslips with DI H2O bottle - use lots of H2O

10) Spritz coverslips with ethanol bottle - use lots of ethanol

11) Repeat steps 5-10 with each rack of coverslips

12) Dry all coverslips in the oven for at least 15 minutes

13) Store coverslips in racks inside sealed plastic nalgene containers

A.5 Glass flow cell

Adapted from David Appleyard

This protocol outlines the construction of the ubiquitous glass flow cell used for optical trap assays.

A typical flow cell will have a volume between 10 and 20 ml if constructed with a 4-5 mm gap.

Materials

1) Etched coverslips A.2

2) Double sided tape (Cat # 909955, Office Depot)

3) Glass slides (Cat # 48312-068, VWR)

Construction procedure

1) Place to pieces of tape along the short axis of the glass slides with approximately 5 mm separating them (the channel width). Remove all overhanging tape.

2) Place an etched coverslip on top of the two pieces of tape. Align the coverslip so that the long axis of the coverslip is perpendicular to the long axis of the glass slide.

3) Use a q-tip or eppendorf tube to gently press the slides together to seal the tape.

4) Initial loading of the flow cell will occur by capilary action

Exchanging flow cell contents

1) Open the vacuum supply line

2) Place the liquid to load on one side of the coverslip in contact with the flow chamber

3) Place the vacuum line nozzle on the other side of the flow chamber and begin to suck the contents through

4) Change the location of the nozzle to control flow through speed

A.6 PEGylation of glass cover slips

Adapted from Yongdae Shin and Marie Aubim-Tam

Materials

600mL acetone

6mL 3-*aminopropyl*triethoxysilane

84mg sodium carbonate ($NaHCO_3$)

40mg PEG-NHS (for making 8 slides)

biotin-PEG-NHS

1) Etch glass cover slips with KOH —see KOH etching protocol

   (if you have slips that have been KOH etched in the previous days, do a plasma etching instead)

Silanisation

2) Place four 1L-beakers in the fume hood:

   Rinse beakers #1 and #2 with acetone and fill them with 300mL acetone.

   Add 6mL of 3-*aminopropyl*triethoxysilane to beaker #2 to make a 2% solution

   Put 300mL of ddH_2O in beakers #3 and #4

3) Transfer slips on "silanisation rack"
4) Put rack of slips in beaker #1 for 5 min
5) Put rack of slips in beaker #2 for 20 min and sonicate for 1 min after the first 10 min
6) Put rack of slips in beaker #3 until no more pearling of water on slips
7) Rinse in beaker #4

8) Dry with forced air and place slips in original rack

PEGylation

Adapted from Yongdae Shin

1) Take bottle of PEG aliquots with desiccants out of -20C freezer and let it equilibrate to room temperature before opening
2) Mix 10mL of ddH_2O with 84 mg of sodium carbonate ($NaHCO_3$)
3) Adjust pH to 8.7 with KOH solution
4) Filter with 0.2μm syringe filter
5) Add 320μL of sodium carbonate solution to aliquots of 40mg of PEG-NHS to obtain concentration of 125g/L
6) Add 88μL of sodium carbonate solution to aliquots of 11mg of biotin-PEG-NHS to obtain concentration of 125g/L
7) Centrifuge 1min at 10,000 RPM to remove bubbles
8) Mix PEG-NHS solution and biotin-PEG-NHS solution in desired ratio
9) Place 80μL of PEG solution on slip and make a sandwich with another slip
10) Incubate 4 hours at room temperature
11) Put slips in "silanisation rack"
12) Put 300mL of ddH_2O in 1L-beaker and rinse rack
13) Dry slips with forced air
14) Keep under vacuum

Appendix B

MATLAB code

Histogram.m

```
Author: Ricardo Gonzalez


clear all

figure;

files = dir('*.mat')
numFiles = length(files);
for i = 1:numFiles;
    nameFile = files(i).name;
    load(nameFile);
    StallForce(i)  = event.StallForce;
end

figure(2)
bin = 10;
[N,X] = hist(StallForce,bin);
Y = N/length(StallForce);
bar(X,Y,0.3,'r')
xlabel('Stall Force (pN)')
title(['Stall Force Distribution - Mean:
',num2str(mean(StallForce)),' pN'])
hold on

xdata1=X;
ydata1=Y;

    xstart=[3.25 1.0 0.5];
    [estimates]=fit_gauss(xdata1,ydata1,xstart);
    A=estimates(1);
    S=estimates(2);
    xplot=0.2*min(xdata1):(max(xdata1)-
0.2*min(xdata1))/100:1.2*max(xdata1);
    yplot=estimates(3)*exp(-((xplot-A).^2)/(2*S^2));

plot(xplot,yplot)
```

```
function [estimates, model] = fit_gauss(xdata,
ydata,start_point)
% Call fminsearch with a random starting point.
% startμpoint = rand(1, 2);
model = @expfun;
estimates = fminsearch(model, startμpoint);
% expfun accepts curve parameters as inputs, and outputs
sse,
% the sum of squares error for A * exp(-lambda * xdata) -
ydata,
% and the FittedCurve. FMINSEARCH only needs sse, but we
want to
% plot the FittedCurve at the end.
    function [sse, FittedCurve] = expfun(params)
        A = params(1);
        S = params(2);
        pmax = params(3);
%         FittedCurve = A .* exp(-lambda * xdata);
        FittedCurve = pmax*exp(-((xdata-A).^2)/(2*S^2));
        ErrorVector = FittedCurve - ydata;
        sse = sum(ErrorVector .^ 2);
    end
end
```

StallForce.m

```
Author: David Appleyard.
Before starting program: (1) Make directory called "events"
%                          (2) Make subdirectories called
"stalls" & "discards"


clear; clc; close all

% Vfile = 'Run5b';
% Calfile = 'CalWTK51';
% StiffFile = 'CalWTK52';

Vfile = 'Run2';
Calfile = 'CalK21';
StiffFile = 'CalK22';


startEvent = 1;
%%%%%%%%%%%%%%%%%%%%%%%%%%%%%%%%%%%%%%%%%%%%%%%%%%%%%%%%%%%%%%%%%%%%%%%%
%%%%%%%%%%
%   Set MT Direction
%%%%%%%%%%%%%%%%%%%%%%%%%%%%%%%%%%%%%%%%%%%%%%%%%%%%%%%%%%%%%%%%%%%%%%%%
%%%%%%%%%%%%%%%%
direct=1; % Either +1 or -1 to make displacements positive

% Threshold force
fcut=1.2;

% Time ahead of the event that is plotted out (sec)
Time_ahead = 5;

%%%%%%%%%%%%%%%%%%%%%%%%%%%%%%%%%%%%%%%%%%%%%%%%%%%%%%%%%%%%%%%%%%%%%%%%
%%%%%%%%%%%%%%%%
%   Read in data
%%%%%%%%%%%%%%%%%%%%%%%%%%%%%%%%%%%%%%%%%%%%%%%%%%%%%%%%%%%%%%%%%%%%%%%%
%%%%%%%%%%%%%%%%

%%%%%%%%%%%%%%%%%%%%%%%%%%%%%%%%%%%%%%%%%%%%%%%%%%%%%%%%%%%%%%%%%%%%%%%%
%Read in for the XY plot version
%Read in data file
tdata=dlmread(Vfile);
len1=length(tdata(:,1));
tme=2000; % Acquisition rate
```

```
%Create matrix with time, Voltage X, Voltage Y
t=0:1/tme:(1/tme*(len1-1));
x=tdata(1:len1,1);
y=tdata(1:len1,2);
%%%%%%%%%%%%%%%%%%%%%%%%%%%%%%%%%%%%%%%%%%%%%%%%%%%%%%%%%%%%


%%%%%%%%%%%%%%%%%%%%%%%%%%%%%%%%%%%%%%%%%%%%%%%%%%%%%%%%%%%%
%%%%%%%%%%%%%%%%
%   Converts the Voltage to Position, then multiplies by
stiffness to get
%   Force.
%%%%%%%%%%%%%%%%%%%%%%%%%%%%%%%%%%%%%%%%%%%%%%%%%%%%%%%%%%%%
%%%%%%%%%%%%%%%%

rawnmdata=ConvertVtoNM(x,y,Calfile);
rawnmdata(:,1:2)=rotateCoords(rawnmdata(:,1:2),-45);

%%%%%%%%%%%%%%%%%%%%%%%%%%%%%%%%%%%%%%%%%%%%%%%%%%%%%%%%%%%%
%%%%%%%%%%%%%%%%
%   Plot the position data and allow user to select a
representative
%   baseline segment.  Subtract the baseline off so that it
is "zeroed"
%%%%%%%%%%%%%%%%%%%%%%%%%%%%%%%%%%%%%%%%%%%%%%%%%%%%%%%%%%%%
%%%%%%%%%%%%%%%%
figure
plot(1:length(rawnmdata(:,1)),rawnmdata(:,1),'-
r',1:length(rawnmdata(:,2)),rawnmdata(:,2),'-b')
xlabel('Index')
ylabel('Position (nm)')
legend('X','Y')
axis tight

fh(1)=gcf;
xlims=get(gca,'XLim'); %get the new x limits

%Create cursors
cnums(1)=CreateCursor(fh(1),'BG 1',[26/255 133/255 5/255]);
cnums(2)=CreateCursor(fh(1),'BG 2',[26/255 133/255 5/255]);

SetCursorLocation(cnums(1),(xlims(2)-xlims(1))/3);
SetCursorLocation(cnums(2),2*(xlims(2)-xlims(1))/3);
```

```
disp('Place cursors to indicate desired regions (BG =
Background)');
input('Hit enter once you are satisfied with your
selection');

for iCnt=1:2
    cps(iCnt)=floor(GetCursorLocation(cnums(iCnt)));
end

xadj=mean(rawnmdata(cps(1):cps(2),1));
yadj=mean(rawnmdata(cps(1):cps(2),2));
rawnmdata(:,1)=(rawnmdata(:,1)-xadj)*direct;
rawnmdata(:,2)=(rawnmdata(:,2)-yadj)*direct;

disp(['Adjusting X baseline by ', num2str(xadj)]);
disp(['Adjusting Y baseline by ', num2str(yadj)]);
close(fh(1));

%%%%%%%%%%%%%%%%%%%%%%%%%%%%%%%%%%%%%%%%%%%%%%%%%%%%%%%%%%%%%%%%%%%%%%%
%%%%%%%%%%%%%%%%
%   Decimating the nmdata and time data
%   Decimation runs a chebyzhev filter on the data - boxcar
might be
%   better?
%%%%%%%%%%%%%%%%%%%%%%%%%%%%%%%%%%%%%%%%%%%%%%%%%%%%%%%%%%%%%%%%%%%%%%%
%%%%%%%%%%%%%%%%

decval=50;  %A 20 decimation should take this to a "100Hz"
sampling
nmdata(:,1)=decimate(rawnmdata(:,1),decval);
nmdata(:,2)=decimate(rawnmdata(:,2),decval);
nmt=decimate(t,decval)';


%%%%%%%%%%%%%%%%%%%%%%%%%%%%%%%%%%%%%%%%%%%%%%%%%%%%%%%%%%%%%%%%%%%%%%%
%%%%%%%%%%%%%%%%
%   Read in the stiffness file, convert to nm space, and
calculate
%   stiffness from the variance method
%%%%%%%%%%%%%%%%%%%%%%%%%%%%%%%%%%%%%%%%%%%%%%%%%%%%%%%%%%%%%%%%%%%%%%%
%%%%%%%%%%%%%%%%

%Parameters
kb=1.3806503*10^-23; %J/K
T=300; %K

stifftrace=dlmread(StiffFile);
```

```
stiff_pos_data=ConvertVtoNM(stifftrace(:,1),stifftrace(:,2)
,Calfile);
stiff_pos_data=rotateCoords(stiff_pos_data,-45);

varx=var((stiff_posμdata(:,1)-
mean(stiff_pos_data(:,1)))*10^-9);
kxvar=(kb*T/(varx)*10^3);%pN/nm

vary=var((stiff_pos_data(:,2)-
mean(stiff_pos_data(:,2)))*10^-9);
kyvar=(kb*T/(vary)*10^3);%pN/nm

disp(['X stiffness is: ',num2str(kxvar),' pN/nm'])
disp(['Y stiffness is: ',num2str(kyvar),' pN/nm'])

%%%%%%%%%%%%%%%%%%%%%%%%%%%%%%%%%%%%%%%%%%%%%%%%%%%%%%%%%%%%%%%%%%%%%%%
%%%%%%%%%%%%%%%%
%   Convert run data to force
%%%%%%%%%%%%%%%%%%%%%%%%%%%%%%%%%%%%%%%%%%%%%%%%%%%%%%%%%%%%%%%%%%%%%%%
%%%%%%%%%%%%%%%%

fdata(:,1)=nmdata(:,1)*kxvar;
fdata(:,2)=nmdata(:,2)*kyvar;


% Rotates data if is off the 45 degree axis by using a
least-squares fit.
%%%%%%%%%%%%%%%%%%%%%%%%%%%%%%%%%%%%%%%%%%%%%%%%%%%%%%%%%%%%%%%%%%%%%%%
%%%%%%%%%%%%%%%%
%   This returns a subplot of X vs. Y after rotation.
%%%%%%%%%%%%%%%%%%%%%%%%%%%%%%%%%%%%%%%%%%%%%%%%%%%%%%%%%%%%%%%%%%%%%%%
%%%%%%%%%%%%%%%%
figure
odeg=FindMTRotationBoxcar(nmdata(:,1),nmdata(:,2));


%Reset data to account for MT orientation
%
%%%%%%%%%%%%%%%%%%%%%%%%%%%%%%%%%%%%%%%%%%%%%%%%%%%%%%%%%%%%%%%%%%%%%%%
%%%%%%%%%%%%%%%%
%   Makes a linear ajustment in position and force with the
rotation.
%%%%%%%%%%%%%%%%%%%%%%%%%%%%%%%%%%%%%%%%%%%%%%%%%%%%%%%%%%%%%%%%%%%%%%%
%%%%%%%%%%%%%%%%
fdata(:,1:2)=rotateCoords(fdata(:,1:2),-1*odeg);
nmdata(:,1:2)=rotateCoords(nmdata(:,1:2),-1*odeg);
```

```
rotrawnmdata(:,1:2)=rotateCoords(rawnmdata(:,1:2),-1*odeg);

%%%%%%%%%%%%%%%%%%%%%%%%%%%%%%%%%%%%%%%%%%%%%%%%%%%%%%%%%%%%%%%%%%%%%%%%%%%%
%%%%%%%%%%%%%%%%%
%   Creates yvel, or velocity in the paralell to MT
position.
%%%%%%%%%%%%%%%%%%%%%%%%%%%%%%%%%%%%%%%%%%%%%%%%%%%%%%%%%%%%%%%%%%%%%%%%%%%%
%%%%%%%%%%%%%%%%%

dt=nmt(2)-nmt(1);
yvel=diff(nmdata(:,2))/dt;
btnum=length(nmdata(:,2));

%%%%%%%%%%%%%%%%%%%%%%%%%%%%%%%%%%%%%%%%%%%%%%%%%%%%%%%%%%%%%%%%%%%%%%%%%%%%
%%%%%%%%%%%%%%%%%
%   The release point is defined by having a high
"snapback" value (>2000
%   nm/s), a high force value (1 pN), and that points are
not next to
%   one another (an anomoly mostly due to averaging).
Finally, the immediate
%   preceding velocity is looked at to determine if slowing
down.  For WT,
%   this value is 200 nm/s, or roughly 1/2 max.  The
analysis went back 10
%   points, or 0.1 sec.  This is enough for 1-2 steps to
occur.  For the
%   heterodimer the max velocity will be 20 nm/s, going
back 100 points
%   (1s).
%%%%%%%%%%%%%%%%%%%%%%%%%%%%%%%%%%%%%%%%%%%%%%%%%%%%%%%%%%%%%%%%%%%%%%%%%%%%
%%%%%%%%%%%%%%%%%

%Snapback velocity cutoff
sncut=500;

%Find points that are above the force and snapback cutoff
releasepoint=(abs(yvel(:))>sncut) & (abs(fdata(1:btnum-
1,2))>fcut);

%Assures that no release points are next to each other
releasepointp=[logical(0)
releasepoint(1:length(releasepoint)-1)'];
releasepoint=logical(releasepoint-
(releasepoint&releasepointp'));

rpindex=find(releasepoint);
```

```
%%%%%%%%%%%%%%%%%%%%%%%%%%%%%%%%%%%%%%%%%%%%%%%%%%%%%%%%%%%%%%%%%%%%%%%
%%%%%%%%%%%%%%
%Readjust the release points to occur at the maximum force
near the
%calculated release point (sometimes these seem to occur in
the midst of
%a drop (may want to change the force cutoff)

%window to look for maximum force +/-
fwindow=10;
for icnt=1:length(rpindex)
    ind=rpindex(icnt);
    if (ind-fwindow)>0 &&
(ind+fwindow)<length(releasepoint)
        [mxval,mxind]=max(fdata((ind-
fwindow):(ind+fwindow),2));
    end
    if fdata(ind,2) < mxval
        releasepoint(ind)=logical(0);
        releasepoint(ind + mxind - fwindow)=logical(1);
    end
end
rpindex=find(releasepoint);
%%%%%%%%%%%%%%%%%%%%%%%%%%%%%%%%%%%%%%%%%%%%%%%%%%%%%%%%%%%%%%%%%%%%%%%
%%%%%%%%%%%%%%%

%%%%%%%%%%%%%%%%%%%%%%%%%%%%%%%%%%%%%%%%%%%%%%%%%%%%%%%%%%%%%%%%%%%%%%%
%%%%%%%%%%%%%%%
%   Plot out the force vs time curve and show where all the
peaks are
%%%%%%%%%%%%%%%%%%%%%%%%%%%%%%%%%%%%%%%%%%%%%%%%%%%%%%%%%%%%%%%%%%%%%%%
%%%%%%%%%%%%%%%
figure
plot(nmt(:),fdata(:,1),'r',nmt(:),fdata(:,2),'b',...
    nmt(releasepoint),fdata(releasepoint,2),'ok')
xlabel('Time (s)')
ylabel('Force (pN)')
hold
for iInt=1:length(rpindex)

text(nmt(rpindex(iInt)),fdata(rpindex(iInt),2)+0.7,num2str(
iInt));
end
title(['Force vs. Time - ',Vfile])
axis tight
```

```
%%%%%%%%%%%%%%%%%%%%%%%%%%%%%%%%%%%%%%%%%%%%%%%%%%%%%%%%%%%%
%%%%%%%%%%%%%%%
%   Extracting individual peaks.
%   Find data where force is above the fcut/2
%   Pull data where force is above the fcut/2 and has a
release point
%   Take X points before and after this region (to get
baselines)
%%%%%%%%%%%%%%%%%%%%%%%%%%%%%%%%%%%%%%%%%%%%%%%%%%%%%%%%%%%%
%%%%%%%%%%%%%%%

Above_force=abs(fdata(1:btnum-1,2))<fcut;
Af_index=find(above_force);

pts_ahead=floor(time_ahead/dt);
pts_behind=floor(.5/dt); %look 5/10ths of a second after

for iCnt=startEvent:length(rpindex)

iµstart=af_index(find(af_index<rpindex(iCnt),1,'last'))-
pts_ahead;
    if i_start <= 0
        i_start = 1;
    end
    i_start=i_start*decval;
    p_start=pts_ahead*decval;

i_end=af_index(find(af_index>=rpindex(iCnt),1))+pts_behind;
    if i_end>length(nmt)
        i_end=length(nmt);
    end
    i_end=i_end*decval;
    p_end=(i_end-i_start)-pts_behind*decval;
    if ~(isempty(i_start)|isempty(i_end))
        disp(['Evaluating event #',num2str(iCnt)])
        ecounter(iCnt,1)=iCnt;
        ecounter(iCnt,2)=i_start;
        ecounter(iCnt,3)=i_end;
        [FV
keep]=EvalEvent(t(i_start:i_end)',rawnmdata(i_start:i_end,:
),...
            [kxvar kyvar],[p_start p_end],odeg,direct,...
            [Vfile(1:length(Vfile)-
4),'_Event_',num2str(iCnt)]);
    else
        ecounter(iCnt,:)=[iCnt 0 0];
    end
```

```
end

%% PC
dlmwrite(['.\events\',Vfile(1:length(Vfile)-
4),'_Event_Indices.txt'],ecounter);

%% MAC
%dlmwrite([Vfile(1:length(Vfile)-
4),'µEventµIndices.txt'],ecounter);

fitlen=9;
rpindex=find(releasepoint);
stallslopes=zeros(length(rpindex),1);

for I = 1:length(rpindex)

    stallslope=polyfit(nmt(rpindex(I)-fitlen:rpindex(I)-
1),nmdata(rpindex(I)-fitlen:rpindex(I)-1,2),1);
    stallslopes(I)=stallslope(1);
end


stalltest=stallslopes<200;
stallpoint=rpindex(stalltest);

%%%%%%%%%%%%%%%%%%%%%%%%%%%%%%%%%%%%%%%%%%%%%%%%%%%%%%%%%%%%%%%%%%%%%%%
%%%%%%%%%%%%%%%%
%   Plots a Force vs. Velocity curve.  Overlaid in blue
circles are the
%   "Releasepoints" that have been described previously.
%%%%%%%%%%%%%%%%%%%%%%%%%%%%%%%%%%%%%%%%%%%%%%%%%%%%%%%%%%%%%%%%%%%%%%%
%%%%%%%%%%%%%%%%

figure
plot(abs(fdata(1:btnum-
1,2)),yvel(:),'k.',abs(fdata(releasepoint,2)),yvel(releasep
oint),'o')
xlabel('Force (pN)')
ylabel('Velocity (nm/s)')
title(['Force vs Velocity - ',Vfile])

%%%%%%%%%%%%%%%%%%%%%%%%%%%%%%%%%%%%%%%%%%%%%%%%%%%%%%%%%%%%%%%%%%%%%%%
%%%%%%%%%%%%%%%%
%   Three figure plots showing Velocity, Position and Force
vs. Time,
%   respectfully.  Overlaid in blue circles are the
"Releasepoints" that
```

```
%   have been described previously.  These circles are
"Stallpoints" in the
%   Force vs. Time plot.
%%%%%%%%%%%%%%%%%%%%%%%%%%%%%%%%%%%%%%%%%%%%%%%%%%%
%%%%%%%%%%%%%%

figure
plot(nmt(releasepoint),yvel(releasepoint),'o',nmt(1:btnum-
1),yvel(:),'k')
xlabel('Time (s)')
ylabel('Velocity (nm/s)')
title(['Velocity vs. Time - ',Vfile])

figure
plot(nmt,nmdata(:,1),'r.',nmt,nmdata(:,2),'k.',...
    nmt(releasepoint),nmdata(releasepoint,2),'o')
xlabel('Time (s)')
ylabel('Position (nm)')
legend('X','Y')
title(['Position vs. Time - ',Vfile])
text(nmt(releasepoint),nmdata(releasepoint,2)+5.0,num2str(a
bs(yvel(releasepoint))));

figure
plot(nmt(:),fdata(:,1),'r',nmt(:),fdata(:,2),'k',...
    nmt(stallpoint),fdata(stallpoint,2),'o')
xlabel('Time (s)')
ylabel('Force (pN)')
hold
text(nmt(releasepoint),fdata(releasepoint,2)+0.2,num2str(st
allslopes));
text(nmt(releasepoint),fdata(releasepoint,2)+0.4,num2str(fd
ata(releasepoint,2)));
title(['Force vs. Time - ',Vfile])

figure
stallforces=fdata(stallpoint,2);
hist(stallforces);
xlabel('Stall Force (pN)')
title(['Stall Force Distribution - Mean:
',num2str(mean(stallforces)),' pN'])
```

fileopennewclamp.m

```
Author: Ricardo Gonzalez Rubio

clear all
close all

%%

datadir = 'C:\Documents and
Settings\Ricardo\Desktop\newforceclampdata\Data\FC031709';
% datadir = 'C:\LabworkDrop\Single
Molecule\2G\newclamp\FC031709';
cd(datadir)
%%
datafile = 'FC031709-0400.dat';
calfile = 'FC031709-0400.cal';


% datafile = 'FC031709-0317.dat';
walkdir = -1;

fid = fopen(datafile, 'r');
data = textscan(fid, '%f %f %f %f %f %f %f %f');
fclose(fid);

%%
%%% Define variables

Vx = data{1};
Vy = data{2};

%%Time vector
l = length(Vy);
tsample = 2000;
t = 0:1/tsample:(1/tsample*(l-1));
%%

AODx = data{3};
AODy = data{4};
Fx = data{5};
Fy = data{6};
RangeX = data{7};
RangeY = data{8};

%%
```

```
%%%Calibration File

% calfile = 'FC031709-0317.cal';

fid = fopen(calfile, 'r');
Cal = textscan(fid, '%f %f' , 'headerlines', 6);

calx = Cal{1};
caly = Cal{2};

%%% Convert Vx and Vy to Position

AODtonmx=1148.1; %[nm/MHz]
AODtonmy=1041.1; %[nm/MHz]

BeadX =
AODtonmx*(calx(1)+calx(2)*Vx+calx(3)*Vy+calx(4)*Vx.^2+calx(
5)*Vy.^2+calx(6)*Vx.^3+calx(7)*Vy.^3+calx(8)*Vx.^4+calx(9)*
Vy.^4+calx(10)*Vx.^5+calx(11)*Vy.^5+calx(12)*Vx.*Vy+calx(13
)*Vx.^2.*Vy+calx(14)*Vx.*Vy.^2+calx(15)*Vx.^3.*Vy+calx(16)*
Vx.^2.*Vy.^2+calx(17)*Vx.*Vy.^3+calx(18)*Vx.^4.*Vy+calx(19)
*Vx.^3.*Vy.^2+calx(20)*Vx.^2.*Vy.^3+calx(21)*Vx.*Vy.^4-26);
BeadY =
AODtonmy*(caly(1)+caly(2)*Vx+caly(3)*Vy+caly(4)*Vx.^2+caly(
5)*Vy.^2+caly(6)*Vx.^3+caly(7)*Vy.^3+caly(8)*Vx.^4+caly(9)*
Vy.^4+caly(10)*Vx.^5+caly(11)*Vy.^5+caly(12)*Vx.*Vy+caly(13
)*Vx.^2.*Vy+caly(14)*Vx.*Vy.^2+caly(15)*Vx.^3.*Vy+caly(16)*
Vx.^2.*Vy.^2+caly(17)*Vx.*Vy.^3+caly(18)*Vx.^4.*Vy+caly(19)
*Vx.^3.*Vy.^2+caly(20)*Vx.^2.*Vy.^3+caly(21)*Vx.*Vy.^4-26);


%%
%%% Rotate by 45 degrees.
angle = deg2rad(-45);

Bead = [BeadX BeadY];
BeadRot = Bead*[cos(angle) -sin(angle); sin(angle)
cos(angle)];

BeadRX = BeadRot(:,1)*walkdir;
BeadRY = BeadRot(:,2)*walkdir;
%%
%%% Trap position
TrapX = (AODx-26.0)*AODtonmx*walkdir;
TrapY = (AODy-26.0)*AODtonmy*walkdir;

%%
```

```
%%% Plotting
%X
figure(1);
plot(t,TrapX, '-r');
hold on
plot(t,BeadRX,'-b');
xlabel('Time (s)')
ylabel('Position(nm)')

figure(2);
plot(t,TrapY, '-r');
hold on
plot(t,BeadRY,'-b');
xlabel('Time (s)')
ylabel('Position(nm)')

%%
%%% Filter Data
BeadRFiltX = sgolayfilt(BeadRX, 0, 11);
BeadRFiltY = sgolayfilt(BeadRY, 0, 11);

figure(3)
plot(t,BeadRFiltY);
hold on
plot(t,TrapY,'-r');
xlabel('Time (s)')
ylabel('Position(nm)'
```

EvalKinesin.m

```
Author: Dave Appleyard

function nuts=EvalKinesin(Vfile,Calfile,stiff_file)

%%%%%%%%%%%%%%%%%%%%%%%%%%%%%%%%%%%%%%%%%%%%%%%%%%%%%%%%%%%%%%%%%%%%
%Read in for the cont acq to spreadsheet
% % %Read in data file
% % tdata=dlmread(Vfile);
% % len1=length(tdata(:,1));
% % tme=tdata(1,1);
% % vdata=zeros((len1-1),3);
% %
% % %Create matrix with time, Voltage X, Voltage Y
% % vdata(:,1)=0:1/tme:(1/tme*(len1-2));
% % vdata(:,2)=tdata(2:len1,1);
% % vdata(:,3)=tdata(2:len1,2);
%%%%%%%%%%%%%%%%%%%%%%%%%%%%%%%%%%%%%%%%%%%%%%%%%%%%%%%%%%%%%%%%%%%%

%%%%%%%%%%%%%%%%%%%%%%%%%%%%%%%%%%%%%%%%%%%%%%%%%%%%%%%%%%%%%%%%%%%%
%Read in for the XY plot version
%Read in data file
%%
tdata=dlmread(Vfile);
len1=length(tdata(:,1));
tme=2000; %Sampling speed had 2000 before
vdata=zeros((len1),3);

%Create matrix with time, Voltage X, Voltage Y
vdata(:,1)=0:1/tme:(1/tme*(len1-1));
vdata(:,2)=tdata(1:len1,1);
vdata(:,3)=tdata(1:len1,2);



%%

%Plot raw voltage data
figure
subplot(2,1,1)
plot(vdata(:,1),vdata(:,2),'r',vdata(:,1),vdata(:,3),'k')
xlabel('Time (s)')
ylabel('Voltage (V)')
legend('X','Y')
title(['Raw Voltage vs Time - ',Vfile])
%%
```

```
%Convert Voltage to NM - now in AODX AODY
nmdata=ConvertVtoNM(vdata(:,2),vdata(:,3),Calfile);

%Reset Axis by rotating Coordinates 45 degrees
%now in PSDX PSDY
nmdata(:,1:2)=rotateCoords(nmdata(:,1:2),-45);

%Run a moving boxcar along the data to filter and average it
BoxcarSize=10; %100;
bcarx=mboxcar(nmdata(:,1),BoxcarSize);
bcary=mboxcar(nmdata(:,2),BoxcarSize);
boxtime=vdata(1:length(bcarx),1);

%%
%Evaluate data to see if the MT was not on the 45 degree
orientation

% Fit to a line
pcoeff = polyfit(bcarx, bcary,1);

slope = pcoeff(1);
int = pcoeff(2);

MTdegfix=90-rad2deg(atan(slope));

disp(['Your data was rotated ',num2str(MTdegfix),' degrees to
account for MT orientation'])

subplot(2,1,2)
plot(bcarx,bcary,'.',bcarx,slope*bcarx+int,'r')

stiff=dlmread(stiff_file)

%Multiply by stiffness to get stiffness data
fdata(:,1)=bcarx*stiff(3);
fdata(:,2)=bcary*stiff(4);


%Reset force data to account for MT orientation
fdata(:,1:2)=rotateCoords(fdata(:,1:2),-1*MTdegfix);

%Reset boxcar data to account for MT orientation
bcar=zeros(length(boxtime),2);
bcar(:,1)=bcarx;
bcar(:,2)=bcary;
```

```
% Rotate data
figure
bcar=rotateCoords(bcar,+1*MTdegfix);


% Plot after rotation
x = bcar(:,1)';
y = bcar(:,2)';


pcoeff = polyfit(x,y,1);

slope = pcoeff(1);
int = pcoeff(2);

plot(x,y,'.',x,slope*x+int,'r')
title(['Rotated']);



%%
%Plot Position Data
figure
plot(boxtime,bcar(:,1),'r',boxtime,bcar(:,2),'k')
xlabel('Time (s)')
ylabel('Position (nm)')
legend('X','Y')
title(['Position vs Time - ',Vfile, ' ', num2str(BoxcarSize),'
pt avg.'])

%Plot Force Data
figure
plot(boxtime,fdata(:,1),'r',boxtime,fdata(:,2),'k')
xlabel('Time (s)')
ylabel('Force (pN)')
legend('X','Y')
title(['Force vs Time - ',Vfile, ' ', num2str(BoxcarSize),' pt
avg.'])
```

Fileopener.m

Author: Ricardo Gonzalez

```
clear; clc; close all;
datadir='C:\LabworkDrop\Single Molecule\2G\0224092G';
cd(datadir);

sampleRate = 5000;  % Hz

[bfn bpn]=uigetfile(datadir,'.txt','Bead Data')
[sfn spn]=uigetfile(datadir,'.txt','StagePos Data')
[tfn tpn]=uigetfile(datadir,'.txt','Trap Data')


fid = fopen([tpn tfn], 'r');
trap = textscan(fid, '%f %f %f %f %f %f %f %f %f',
'headerlines', 1);
fclose(fid);

fid = fopen([bpn bfn], 'r');
bead = textscan(fid, '%f %f', 'headerlines', 1);
fclose(fid);

fid = fopen([spn sfn], 'r');
stage = textscan(fid, '%f %f %f', 'headerlines', 1);
fclose(fid);

% ttrap=trap{1};
AODx=trap{2};
AODy=trap{3};
forceangle=trap{4};
Force=trap{5};
offsetx=trap{6};
offsety=trap{7};
TrapPosx=trap{8};
TrapPosy=trap{9};

xpos=bead{1};
ypos=bead{2};

tstage=stage{1};
Stageposx=stage{2};
Stageposy=stage{3};

sampleRate =floor(length(tstage)*100000/(max(tstage)-
min(tstage)));
```

```
tpos = [0:1/sampleRate:(1/sampleRate*(length(ypos)-1))]';
ttrap =
[0:1/(sampleRate/20):(1/(sampleRate/20)*(length(TrapPosy)-1))]';
```

References

1. Khalil, A.S., et al., *Kinesin's cover-neck bundle folds forward to generate force.* Proc Natl Acad Sci U S A, 2008. **105**(49): p. 19247-52.
2. Lang, M.J., et al., *An automated two-dimensional optical force clamp for single molecule studies.* Biophys J, 2002. **83**(1): p. 491-501.
3. Svoboda, K. and S.M. Block, *Biological applications of optical forces.* Annu Rev Biophys Biomol Struct, 1994. **23**: p. 247-85.
4. Appleyard, D., *Engineering Optical Traps for New Environments and Applications in the Measurements of Biological Adhesives and Motors.* Doctoral Thesis, 2008(MIT).
5. Hwang, W. and M.J. Lang, *Mechanical design of translocating motor proteins.* Cell Biochem Biophys, 2009. **54**(1-3): p. 11-22.
6. Khalil, A., *Biology's Wires and Motors: Single-Molecule Mechanics of M13 Bacteriophage and Kinesin.* MIT Thesis, 2009.
7. Lang, M.J., *Lighting up the Mechanome.* The Bridge, 2007. **37** (4): 11-16.
8. Neuman, K.C. and A. Nagy, *Single-molecule force spectroscopy: optical tweezers, magnetic tweezers and atomic force microscopy.* Nat Methods, 2008. **5**(6): p. 491-505.
9. Schnitzer, M.J. and S.M. Block, *Kinesin hydrolyses one ATP per 8-nm step.* Nature, 1997. **388**(6640): p. 386-90.
10. Ashkin, A., *Forces of a single-beam gradient laser trap on a dielectric sphere in the ray optics regime.* Biophys J, 1992. **61**(2): p. 569-582.
11. Neuman, K.C. and S.M. Block, *Optical trapping.* Rev Sci Instrum, 2004. **75**(9): p. 2787-809.
12. Herbert, K.M., W.J. Greenleaf, and S.M. Block, *Single-molecule studies of RNA polymerase: motoring along.* Annu Rev Biochem, 2008. **77**: p. 149-76.

13. Cheezum, M.K., W.F. Walker, and W.H. Guilford, *Quantitative comparison of algorithms for tracking single fluorescent particles.* Biophys J, 2001. **81**(4): p. 2378-88.

14. Berg-Sorensen, K. and H. Flyvbjerg, *Power spectrum analysis for optical tweezers.* Review of Scientific Instruments, 2004. **75**(3): p. 594-612.

15. Sheetz, M.P., *Laser tweezers in cell biology. Introduction.* Methods Cell Biol, 1998. **55**: p. xi-xii.

16. Block, S.M., et al., *Probing the kinesin reaction cycle with a 2D optical force clamp.* Proc Natl Acad Sci U S A, 2003. **100**(5): p. 2351-6.

17. Lawrence, C.J., et al., *A standardized kinesin nomenclature.* J Cell Biol, 2004. **167**(1): p. 19-22.

18. Mandelkow, E. and E.M. Mandelkow, *Kinesin motors and disease.* Trends Cell Biol, 2002. **12**(12): p. 585-91.

19. Ohira, M., et al., *Identification and characterization of a 500-kb homozygously deleted region at 1p36.2-p36.3 in a neuroblastoma cell line.* Oncogene, 2000. **19**(37): p. 4302-7.

20. Hakimi, M.A., D.W. Speicher, and R. Shiekhattar, *The motor protein kinesin-1 links neurofibromin and merlin in a common cellular pathway of neurofibromatosis.* J Biol Chem, 2002. **277**(40): p. 36909-12.

21. Vale, R.D., *The molecular motor toolbox for intracellular transport.* Cell, 2003. **112**(4): p. 467-80.

22. Block, S.M., *Kinesin: what gives?* Cell, 1998. **93**(1): p. 5-8.

23. Yildiz, A. and P.R. Selvin, *Kinesin: walking, crawling or sliding along?* Trends Cell Biol, 2005. **15**(2): p. 112-20.

24. Vale, R.D. and R.A. Milligan, *The way things move: looking under the hood of molecular motor proteins.* Science, 2000. **288**(5463): p. 88-95.

25. Howard, J., *Mechanics of Motor Proteins and the Cytoskeleton.* 2001: Sinauer.

26. Block, S.M., *Kinesin motor mechanics: binding, stepping, tracking, gating, and limping.* Biophys J, 2007. **92**(9): p. 2986-95.

27. Hwang, W., M.J. Lang, and M. Karplus, *Force generation in kinesin hinges on cover-neck bundle formation.* Structure, 2008. **16**(1): p. 62-71.

28. Mandelkow, E. and K.A. Johnson, *The structural and mechanochemical cycle of kinesin.* Trends Biochem Sci, 1998. **23**(11): p. 429-33.

29. Guydosh, N.R. and S.M. Block, *Backsteps induced by nucleotide analogs suggest the front head of kinesin is gated by strain.* Proc Natl Acad Sci U S A, 2006. **103**(21): p. 8054-9.

30. Wang, M.D., et al., *Force and velocity measured for single molecules of RNA polymerase.* Science, 1998. **282**(5390): p. 902-7.

31. Fisher, M.E. and A.B. Kolomeisky, *Simple mechanochemistry describes the dynamics of kinesin molecules.* Proc Natl Acad Sci U S A, 2001. **98**(14): p. 7748-53.

32. Valentine, M.T., P.M. Fordyce, and S.M. Block, *Eg5 steps it up!* Cell Div, 2006. **1**: p. 31.

33. Mori, T., R.D. Vale, and M. Tomishige, *How kinesin waits between steps.* Nature, 2007. **450**(7170): p. 750-4.

34. Lowe, J., et al., *Refined structure of alpha beta-tubulin at 3.5 A resolution.* J Mol Biol, 2001. **313**(5): p. 1045-57.

35. Lakamper, S. and E. Meyhofer, *The E-hook of tubulin interacts with kinesin's head to increase processivity and speed.* Biophys J, 2005. **89**(5): p. 3223-34.

36. Wang, Z. and M.P. Sheetz, *The C-terminus of tubulin increases cytoplasmic dynein and kinesin processivity.* Biophys J, 2000. **78**(4): p. 1955-64.

37. Thorn, K.S., J.A. Ubersax, and R.D. Vale, *Engineering the processive run length of the kinesin motor.* J Cell Biol, 2000. **151**(5): p. 1093-100.

38. Romberg, L., D.W. Pierce, and R.D. Vale, *Role of the kinesin neck region in processive microtubule-based motility.* J Cell Biol, 1998. **140**(6): p. 1407-16.

39. Lakamper, S., et al., *Single fungal kinesin motor molecules move processively along microtubules.* Biophys J, 2003. **84**(3): p. 1833-43.

40. Skiniotis, G., et al., *Modulation of kinesin binding by the C-termini of tubulin.* EMBO J, 2004. **23**(5): p. 989-99.

41. Rasnik, I., et al., *DNA-binding orientation and domain conformation of the E. coli rep helicase monomer bound to a partial duplex junction: single-molecule studies of fluorescently labeled enzymes.* J Mol Biol, 2004. **336**(2): p. 395-408.